crystals

MDPI

Review

On the Coordination Role of Pyridyl-Nitrogen in the Structural Chemistry of Pyridyl-Substituted Dithiocarbamate Ligands

Edward R.T. Tiekink

Research Centre for Crystalline Materials, School of Medical and Life Sciences, Sunway University, Bandar Sunway 47500, Selangor Darul Ehsan, Malaysia; edwardt@sunway.edu.my; Tel.: +60-3-7491-7181

Abstract: A search of the Cambridge Structural Database was conducted for pyridyl-substituted dithiocarbamate ligands. This entailed molecules containing both an NCS_2^- residue and pyridyl group(s), in order to study their complexation behavior in their transition metal and main group element crystals, i.e., d- and p-block elements. In all, 73 different structures were identified with 30 distinct dithiocarbamate ligands. As a general observation, the structures of the transition metal dithiocarbamates resembled those of their non-pyridyl derivatives, there being no role for the pyridyl-nitrogen atom in coordination. While the same is true for many main group element dithiocarbamates, a far greater role for coordination of the pyridyl-nitrogen atoms was evident, in particular, for the heavier elements. The participation of pyridyl-nitrogen in coordination often leads to the formation of dimeric aggregates but also one-dimensional chains and two-dimensional arrays. Capricious behaviour in closely related species that adopted very different architectures is noted. Sometimes different molecules comprising the asymmetric-unit of a crystal behave differently. The foregoing suggests this to be an area in early development and is a fertile avenue for systematic research for probing further crystallization outcomes and for the rational generation of supramolecular architectures.

Keywords: thiolate ligands; dithiocarbamate ligands; pyridyl; coordination chemistry; coordination polymers; metal clusters; crystal structures

Citation: Tiekink, E.R.T. On the Coordination Role of Pyridyl-Nitrogen in the Structural Chemistry of Pyridyl-Substituted Dithiocarbamate Ligands. *Crystals* **2021**, *11*, 286. https://doi.org/10.3390/cryst11030286

Academic Editor: Alexander Kirillov

Received: 2 March 2021
Accepted: 11 March 2021
Published: 14 March 2021

1. Introduction

In their most common form, dithiocarbamate ligands are mono-anionic ligands of the general formula $^-S_2CNR_2$, for R = alkyl, aryl. These are readily prepared from the reaction of a secondary amine and carbon disulfide in the presence of a base, for example, an alkali hydroxide. The dithiocarbamates are clearly the most important member of the 1,1-dithiolate class of ligands, and have been known for 150 years or thereabouts [1,2]. The motivations for studying metal complexes of dithiocarbamates (and their diseleno-analogues), including their main group element and lanthanide compounds, are many and varied, as summarized in a number of reviews published over the last 50 years [3–8]. Notwithstanding the utility of dithiocarbamates in materials chemistry, medicine, lubricating oils, etc., here, the focus is upon the structural chemistry of a specific class of multi-functional dithiocarbamate ligands, namely pyridyl-substituted dithiocarbamate ligands.

Generally, the reaction to form $^-S_2CNR_2$ is facile and the range of ligands that can be generated is only limited by the availability of the amine, both secondary (Scheme 1, Equation (1)) and primary (Scheme 1, Equation (2)), where the latter generates $^-S_2CN(H)R$; the coordination chemistry of $^-S_2CNH_2$ is relatively limited [6,7]. While dissymmetric secondary amines can lead to $^-S_2CNRR'$, further broadening of the range of the available dithiocarbamate ligands for investigation can be achieved by functionalizing the amine substituents to give rise to multi-functional dithiocarbamate ligands. A relevant example of this idea is the reaction of piperazine with two equivalents of carbon disulfide to form the piperazine bis(dithiocarbamate) ligand, i.e., $^-S_2CN(CH_2CH_2)_2NCS_2^-$. Complexation of this with metal salts can be anticipated to result in di-nuclear molecules, and experience

suggests that the methods and handling of reactants, reactions, and products for this synthesis presents no special difficulties [9]. Indeed, very recently, a review of the coordination chemistry of such poly-functional dithiocarbamate ligands was published [10].

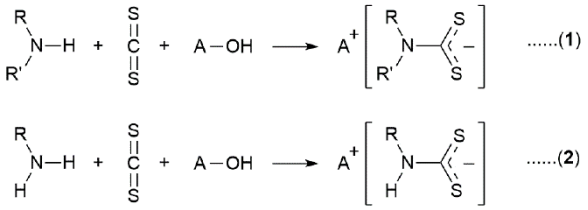

Scheme 1. Preparation of dithiocarbamate ligands from secondary (Equation (1)) and primary (Equation (2)) amines. R, R′ = alkyl, aryl, and A = alkali metal or ammonium salt.

This aforementioned survey [10] reported 40 poly-functional dithiocarbamate ligands that were characterized by the crystal structures of their metal complexes. While the overwhelming majority of poly-functional dithiocarbamates carried two NCS_2^- residues, there were examples of ligands with three, four, and up to six NCS_2^- residues. In terms of coordination chemistry, while many of the resultant coordination complexes were relatively simple di-nuclear species, higher nuclearity aggregates, up to an impressive 36 (gold) atoms [11], were noted. Less common were one- and two-dimensional architectures with a sole example of a three-dimensional architecture adopted by a series of isostructural lanthanide-based materials [12]. Naturally, the functionalization of amines could proceed beyond additional amine functionality, such as in multi-functional dithiocarbamate ligands bearing carboxylic groups. However, despite being known since the 1980's, with the preparation of barium salts of various dithiocarbamates derived from amino acids [13], the chemistry of this potentially interesting class of ligands remains relatively unexplored [14]. In contrast, considerably more attention was directed towards the study of dithiocarbamate ligands, bearing at least one neutral pyridyl residue, and this chemistry formed the focus of the present survey.

Herein, a bibliographic survey of the reported crystal structures of transition metal (d-block elements) and main group element (p-block elements that form the majority of examples) dithiocarbamates that also present pyridyl group(s) available for further coordination is presented. Brief comments on the context behind their syntheses is also given when pertinent, as well as a comparison with their non-functionalized analogues.

2. Methods

The present bibliographic review of the crystallographic literature is based on a systematic search of the Cambridge Structural Database (CSD, version 5.41 + three updates) [15] employing ConQuest (version 2.0.4) [16]. The search involved an evaluation of all structures containing an NCS_2 residue, plus a pyridyl group. No other restrictions were applied. Each of the 493 retrieved structures was manually screened, leading to 73 independent crystal structures of coordinated pyridyl-substituted dithiocarbamate ligands. A total of 30 different ligands were noted, many were isomers or differ only in a minor way, such as in the nature of the remote substituents; their chemical diagrams with abbreviations are given in Figure 1. The composition details for each crystal are given in Table 1, as well as the CSD REFCODE and literature citation. All crystallographic diagrams are original and were generated by employing DIAMOND [17], using the data included in the Crystallographic Information File obtained from the CSD for each structure.

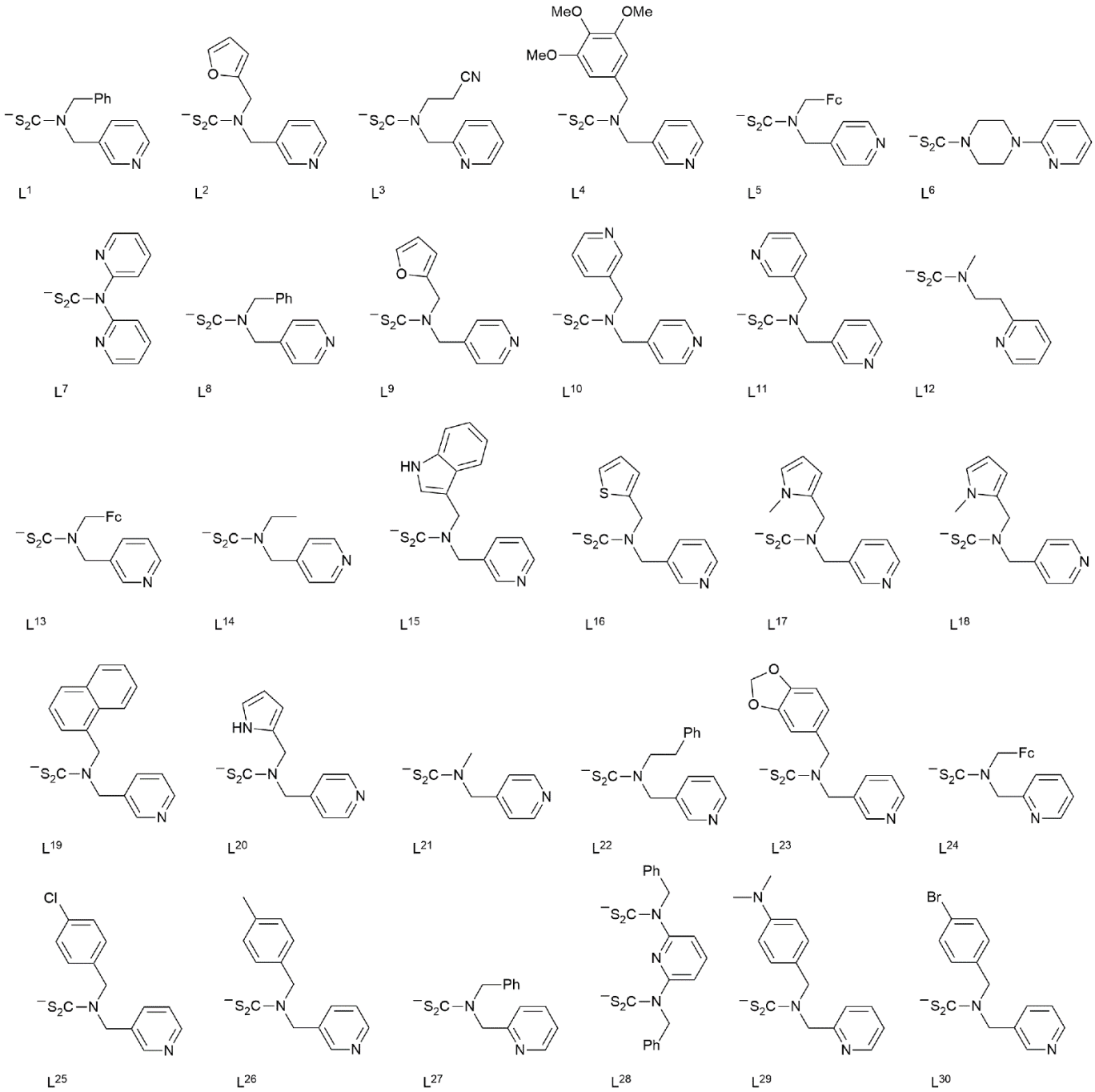

Figure 1. Chemical diagrams for pyridyl-functionalized dithiocarbamate anions L^1 to L^{30}. Fc = $(C_5H_4)Fe(C_5H_5)$, ferrocenyl.

Table 1. Summary of structures **1**–**73** discussed in this bibliographic review.

Crystal	Formulation	Motif	CSD REFCODE	Ref.
1	$Ni(L^1)_2$	monomer	DEXFIX	[18]
2	$Ni(L^2)_2$	monomer	DIFHIL	[18]
3	$Ni(L^3)_2$	monomer	HUTNOB	[19]
4	$Ni(L^4)_2$	monomer	LUKTIW	[20]
5 [a]	$(NN^1)Ni(L^5)$	monomer	VOTDEP	[21]
6	$Pd(L^1)_2$	monomer	HOMXEO	[22]

Table 1. *Cont.*

Crystal	Formulation	Motif	CSD REFCODE	Ref.
7	$[(4\text{-tol})_3P]Pd(L^6)Cl$	monomer	ROHKAD	[23]
8	$Pt(L^1)_2$	monomer	LASPIH	[24]
9	$Pt(L^7)_2$	monomer	UHOGIJ	[25]
10	$[(4\text{-tol})_3P]Pt(L^6)Cl$	monomer	RIZNEW	[26]
11	$Cu(L^1)_2$	monomer	MISLUX	[27]
12	$Cu(L^7)_2$	monomer	ZUWLUY	[28]
13	$(Ph_3P)_2Cu(L^8).2H_2O$	monomer	LEBDIH	[29]
14	$(Ph_3P)_2Cu(L^9)$	monomer	NOJVIT	[30]
15	$(Ph_3P)_2Cu(L^{10}).0.5(CH_2Cl_2).0.5(H_2O)$	monomer	MORNIT	[31]
16	$[(Ph_3P)_2Ag(L^1)]_2$	dimer	GONMED	[32]
17	$[(Ph_3P)_2Ag(L^{11})]_2$	dimer	GONMIH	[32]
18	$[Ag(L^1)]_n$	1-D	GONLUS	[32]
19	$[Ag(L^{11})]_n$	1-D	GONMAZ	[32]
20	$[Au(L^7)]_2$	monomer	XIRYII	[33]
21	$[Au(L^{12})]_2$.isophthalic acid	monomer	EYURAS	[34]
22	$[Zn(L^1)_2]_2$.EtOH	dimer	FODSIC	[35]
23	$[Zn(L^{13})_2]_2$	dimer	UTEJOU	[36]
24	$[Zn(L^{14})_2]_n$.0.5(4-methylpyridine)	1-D	FECRIR	[37]
25	$[Zn(L^5)_2]_2$.2(DMF)	2-D	UTEJUA	[36]
26	$Cd(L^{13})_2$(2,2′-bipyridyl)	monomer	GIVGUQ	[38]
27	$Cd(L^{13})_2$(1,10-phenanthroline)	monomer	GIVGOK	[38]
28	$Cd(L^{14})_2$(1,10-phenanthroline)	monomer	UTEKIP	[36]
29	$[Cd(L^{15})]_2$.2(DMF)	dimer	ZODSUI	[39]
30	$[Cd(L^{14})]_n$.3-methylpyridine	2-D	GAMVAU	[40]
31	$[Cd(L^1)]_n$	2-D	ZODSAO	[39]
32	$[Cd(L^{11})]_n$	2-D	ZODSES	[39]
33	$[Cd(L^{16})]_n$	2-D	ZODSOC	[39]
34	$[Cd(L^{13})]_n$.acetonitrile	2-D	UTEKAH	[36]
35	$[Cd(L^2)]_n$	2-D	ZODSIW	[39]
36	$Hg(L^1)_2$	monomer	FODSAU	[35]
37	$Hg(L^8)_2$	monomer	EBUTAY	[41]
38	$Hg(L^{17})_2$	monomer	XOBCEY	[42]
39	$Hg(L^{18})_2$	monomer	YOMYOQ	[43]
40	$[Hg(L^{13})_2]_2$	dimer	UTEKEL	[36]
41	$[Hg(L^{19})_2]_2$·MeOH	dimer	XOBCAU	[42]
42	$PhHg(L^5)$	dimer	EKIYON	[44]
43	$PhHg(L^{17})$	dimer	XOBBOH	[42]
44	$PhHg(L^{20})$·2(MeOH)	dimer	FODRUN	[35]
45	$[PhHg(L^{18})]_2$	dimer	YOMYAC	[43]
46	$[PhHg(L^{21})]_2$	dimer	EBUSOL	[41]
47	$[Hg(L^{10})_2]_n$	1-D	YOMYIK	[43]
48	$[Hg(L^{22})_2]_n$	1-D	FODROH	[35]
49	$[Hg(L^{21})_2]_n$	1-D	FODREX	[35]
50	$[Hg(L^{23})_2]_n$	1-D	FODRAT	[35]
51	$[Hg(L^9)_2]_n$	2-D	FODRIB	[35]
52	$[PhHg(L^8)]_n$	2-D	EBUSIF	[41]
53	$[Tl(L^{24})]_n$	1-D	FEGHEH	[45]
54	$[Tl(L^1)]_n$	2-D	GOQHUR	[46]
55	$[Tl(L^{11})]_n$	2-D	GOQJED	[46]
56	$[Tl(L^{13})]_n$	2-D	GOQKAA	[46]
57	$[Tl(L^{23})]_n$	2-D	GOGJON	[46]
58	$[Tl(L^{16})]_n$	2-D	FEGHOR	[45]
59	$[Tl(L^{25})]_n$	2-D	FEGHUX	[45]
60	$[Tl(L^{26})]_n$	2-D	FEGJAF	[45]
61	$(nBu)_2Sn(L^8)_2$	monomer	UGEFAP	[47]

Table 1. *Cont.*

Crystal	Formulation	Motif	CSD REFCODE	Ref.
62	$(nBu)_2Sn(L^{14})_2$	monomer	CEHKUX	[48]
63	$Ph_2Sn(L^{1})_2$	monomer	UGEFET	[47]
64	$Ph_2Sn(L^{14})_2$	monomer	CEHLAE	[48]
65	$Ph_3Sn(L^{27})$	monomer	TOHBOJ	[49]
66	$[Ph_3Sn]_2(L^{28})$	dimer	TOHGEE	[49]
67	$[(PhCH_2)_2Sn)(L^{28})]_2{\cdot}CH_2Cl_2$	dimer	TOHBUP	[49]
68	$[Me_2Sn(L^{14})_2]_2$	dimer	CEHKOR	[48]
69	$[Ph_3Sn(L^{11})]_n$	1-D	UGEFIX	[47]
70	$[Bi(L^{6})_3]_2$	dimer	JURXAX	[50]
71	$[Bi(L^{25})_3]_2$	dimer	NOTTIC	[51]
72	$[Bi(L^{29})_3]_2$	dimer	NOTTOI	[51]
73	$[Bi(L^{30})_3]_n{\cdot}0.5(HCl)$	1-D	NOTTUO	[51]

[a] $(NN^1)H$ is N,N-dimethyl-4-[1H-pyrrol-2-yl(pyrrol-2-ylidene)methyl]aniline

3. Results

The full chemical composition for each crystal discussed herein, i.e., **1**–**73** [18–51], is included in Table 1: for the purposes of the following description of structures, counter-ions, co-crystal co-formers and solvents are ignored, unless they were pertinent to the coordination modes adopted by the dithiocarbamate ligands or supramolecular aggregation. The ensuing discussion is arranged in terms of the Group of the Periodic Table and in order of lightest to heaviest element. Generally, within each category, homoleptic structures are discussed before organometallic species and other formulations, and the description of structures are in the order of increasing nuclearity of the aggregate, i.e., monomeric species before dimeric species, etc.

3.1. Structures of the Nickel-Triad Elements

There were four homoleptic nickel(II) complexes and each essentially adopted the same structural motif, namely a square–planar geometry defined by an S_4 donor set. The complexes were formulated as $Ni(L^x)_2$, where x = 1 (**1**) [18], x = 2 (**2**) [18], x = 3 (**3**) [19], and x = 4 (**4**) [20] with that of **3**, which was representative of these (illustrated in Figure 2a); the nickel atom was located on a crystallographic site of inversion in each of **1**–**4**. The dithiocarbamate ligand coordinated in a symmetrically chelating mode [Ni–S: 2.20 & 2.21 Å] with no role for the pyridyl-nitrogen atoms in coordination being apparent. This observation, at least for some of the transition metal complexes to be described herein, related to the very nature of the dithiocarbamate ligand itself, in that the contribution of the dithiolate canonical form, i.e., $R_2N^{(+)}{=}CS_2^{(2-)}$, to the overall electronic structure was significant, approaching 40%. This confirmed the very strong bidentate coordination mode of the dithiocarbamate ligand towards metals that reduced the Lewis acidity of the metal center and, in turn, reduced the propensity of the metal to increase its coordination number via interaction with donors such as pyridyl-nitrogen [52].

The interest in several of these structures related to their propensity to form unusual C–H$\cdots$Ni anagostic interactions that were shown to be dependent on the nature of the substituents [18,20,53]. The other non-standard, non-covalent interaction observed in over 35% of the crystals of square–planar nickel(II) dithiocarbamate complexes was the formation of stabilizing intermolecular C–H$\cdots\pi(NiS_2C)$ interactions [54]. This was also accounted for in terms of the prevalence of the aforementioned canonical structure that ensured considerable delocalization of π-electron density over the four-membered (NiS_2C) chelate ring, making this a good acceptor for such interactions, as for any π-system.

The remaining nickel(II) complex was $(NN^1)Ni(L^5)$ (**5**) [21], where $(NN^1)H$ was N,N-dimethyl-4-[1H-pyrrol-2-yl(pyrrol-2-ylidene)methyl]aniline, and is represented in Figure 2b; the dithiocarbamate ligand was chelating in nature [2.19 & 2.21 Å]. This complex was designed specifically to form C–H$\cdots\pi(NiS_2C)$ interactions in the crystal, which were noted [21].

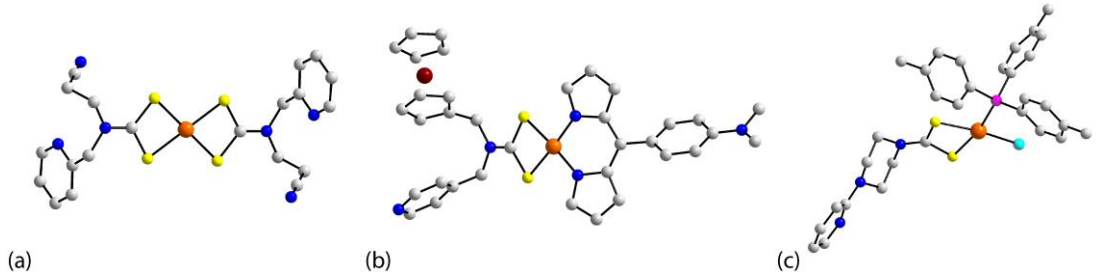

Figure 2. Molecular structures for (**a**) Ni(L^3)$_2$ (**3**), (**b**) (NN^1)Ni(L^5) (**5**), and (**c**) [(4-tol)$_3$P]Pd(L^6)Cl (**7**). Color code in this and subsequent diagrams—the central metal atom is shown in orange; other heavy element, brown; chloride, cyan; sulfur, yellow; phosphorus, purple; nitrogen, blue; and carbon, grey. Generally, hydrogen atoms are omitted for clarity.

Only two palladium(II) structures are known, namely Pd(L^1)$_2$ (**6**) [22], which is isostructural with **1**, and [(4-tol)$_3$P]Pd(L^6)Cl (**7**) [23], a new structural motif to be described. In **7**, Figure 2c, one dithiocarbamate ligand was substituted with chloride and phosphane atoms so a $ClPS_2$ square–planar geometry resulted; the dithiocarbamate ligand chelated the palladium atom, forming dissymmetric Pd–S bond lengths [2.35 & 2.39 Å]. No evidence for Pd$\cdots$N interactions was noted.

There were two homoleptic platinum(II) complexes, i.e., Pt(L^1)$_2$ (**8**) [24], isostructural with **1** and **6**, and Pt(L^7)$_2$ (**9**) [25]. Complex **9** was of particular note as it was the first example having two pyridyl donors per dithiocarbamate ligand. The coordination geometry for [(4-tol)$_3$P]Pt(L^6)Cl (**10**) [26] was as for **7**, Figure 2c. Interest in **7** and **10** relate to investigations of anti-cancer potential, as both species were more active than cisplatin, at least based on in vitro screening, and preliminary SAR pointed to an advantage of L^6.

3.2. Structures of the Copper-Triad Elements

The two homoleptic copper(II) complexes in this section were Cu(L^1)$_2$ (**11**) [27] and Cu(L^7)$_2$ (**12**) [28]; **11** featured two independent molecules in the asymmetric-unit and was investigated as a part of a wider series for electrochemical, conducting, and dielectric properties [27]. Each copper(II) center existed in the expected square–planar geometry within an S_4 donor set [Cu-S: 2.30 to 2.31 Å]. Of interest, and as highlighted in Figure 3a for **12**, the molecules approached each other over a center of inversion, to enable the formation of close Cu$\cdots$S contacts. The Cu$\cdots$S contact of 3.23 Å was just beyond the sum of the van der Waals radii for copper and sulfur, at 3.20 Å [55]. For **11**, one molecule approached the other in a side-on manner and only one Cu$\cdots$S was formed at a rather long separation of 3.58 Å. The formation of intermolecular interactions proved a potential for related interactions with nitrogen but, more decisively, pointed to a competition between sulfur and nitrogen, as borne out in several instances later in the survey.

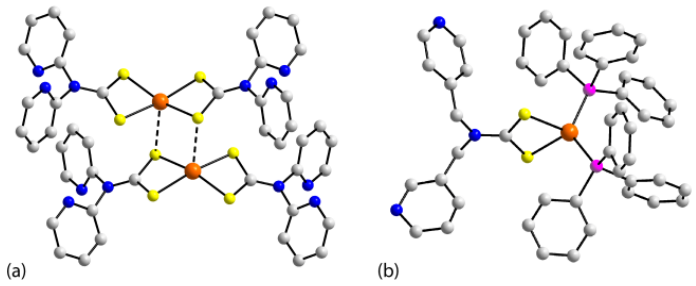

Figure 3. Molecular structures for (**a**) Cu(L^7)$_2$ (**12**) (showing supramolecular association via Cu$\cdots$S interactions between centrosymmetrically-related molecules) and (**b**) (Ph$_3$P)$_2$Cu(L^{10}) (**15**).

The three remaining copper complexes conformed to the general formula (Ph$_3$P)$_2$Cu(L^x) for x = 8 (**13**) [29], x = 9 (**14**) [30] and x = 10 (**15**) [31]. The dithiocarbamate ligand in **15** was particularly notable not only for having two pyridyl substituents but for them

being dissymmetric, i.e., containing 3- and 4-pyridyl residues. All three complexes were strongly luminescent [29–31] with **13**, in particular, exhibiting a blue–green emission at 480 nm. Further, **15** proved to be an efficient catalyst for the generation of "glycoconjugate triazoles under Click protocol" [31]. The complexes conformed to the same structural motif as exemplified in Figure 3b for **15**. The copper(I) atom was coordinated in a distorted tetrahedral geometry, by a symmetrically chelating dithiocarbamate ligand [2.40 & 2.41 Å] and two phosphorus donors. This was the uniformly adopted structural motif for these molecules according to a recent survey [56]. With such a congested environment about the central atom, it was not surprising that additional contacts involving copper and pyridyl-nitrogen atoms were not apparent.

Attention was now directed towards silver, for which the first examples of coordination polymers appeared. The first two complexes were related to monomeric **13**–**15** but were formulated as di-nuclear $[(Ph_3P)Ag(L^x)]_2$ with x = 1 (**16**) and x = 11 (**17**) [32]. Their study indicated some semi-conductor behavior and striking luminescent characteristics in the solid-state. The di-nuclear molecules, represented by **17** in Figure 4a, arose as the dithiocarbamate ligand simultaneously chelated one silver(I) atom [2.63 & 2.72 Å] and bridged to the second [2.68 Å], centrosymmetrically related silver(I) atom. The distorted PS_3 donor set was completed by the phosphorus atom. Again, no evidence for Ag···N interactions was found. Indeed, the structures closely resembled those found for non-functionalized dithiocarbamate ligands [57], of interest owing to anti-bacterial activity. In the absence of phosphane ligands, one-dimensional coordination polymers were formed for the isostructural x = 1 (**18**) and x = 11 (**19**) species formulated as $[Ag(L^x)]_n$. Two images for the exemplar complex **18** are given in Figure 4b. The dithiocarbamate ligand was tridentate, bridging two silver atoms via one sulfur atom [2.59 & 2.64 Å], while linking a third silver atom via the second sulfur atom [2.65 Å]. The interactions perpetuated to form a helical supramolecular chain being propagated by 4_1-screw symmetry. This arrangement allowed for the formation of intra-chain Ag···Ag contacts, which in the case of **18** amounted to 2.89 Å; for **19**, the Ag···Ag separation was 2.85 Å. A simplified view of the chain along the axis of propagation in **18** is shown in the right-hand image of Figure 4b. Metal···metal interactions, this time involving gold, were also noted in the two examples of gold(I) structures to be discussed next.

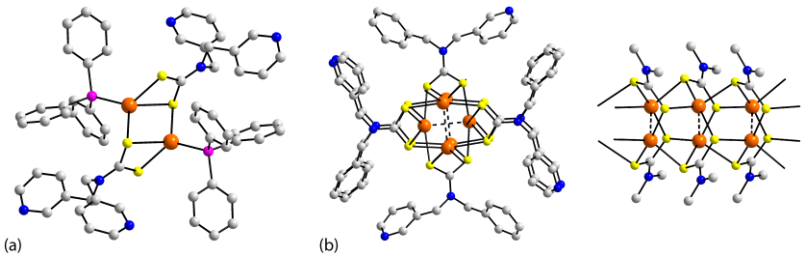

Figure 4. (**a**) Molecular structure for $[(Ph_3P)Ag(L^{11})]_2$ (**17**) and (**b**) two views of the 1-D supramolecular chain in $[Ag(L^1)]_n$ (**18**); in the right-hand image, all but the α-carbon atoms of the dithiocarbamate residues were removed. The dashed lines indicate M···M interactions, in this case M = Ag with the separation being 2.89 Å.

Two independent molecules comprised the asymmetric-unit of $[Au(L^7)]_2$ **20** [33] and each was disposed about a center of inversion to generate the di-nuclear molecule shown in Figure 5a; the second molecule was essentially identical. Here, two gold(I) atoms were bridged by two dithiocarbamate ligands [2 × 2.29 Å; 2.28 & 2.29 Å for the second independent molecule] to form a close to planar, eight-membered {–AuSCS}$_2$ ring. Within the ring, an Au···Au (aurophilic) interaction of 2.79 Å was noted; for the second molecule, Au···Au was 2.82 Å. In the crystal, weak Au···S interactions at separations just beyond the van der Waals radii were noted; these served to link the molecules into a twisted supramolecular chain (not shown). A similar di-nuclear molecule was noted in the crystal of **21** [34], which along with $[Au(L^{12})]_2$ contained one equivalent of isophthalic acid. Both

studies [33,34] were motivated by investigations of the solid-state luminescence attributes of the gold dimers, a well-documented phenomenon for gold thiolates [58]. There were two independent formula units of $[Au(L^{12})]_2$ in **21**, neither with symmetry [Au–S: 2.28 to 2.30 Å]. The transannular Au···Au separations were 2.75 and 2.78 Å. In the crystal, by virtue of hydroxyl-O–H···N(pyridyl) hydrogen-bonding, known to be a persuasive supramolecular synthon [59], the di-nuclear molecules were connected into a twisted supramolecular chain, as shown in Figure 5b; see [60] for a review on the competition between conventional hydrogen bonding and aurophilic interactions in supramolecular chemistry.

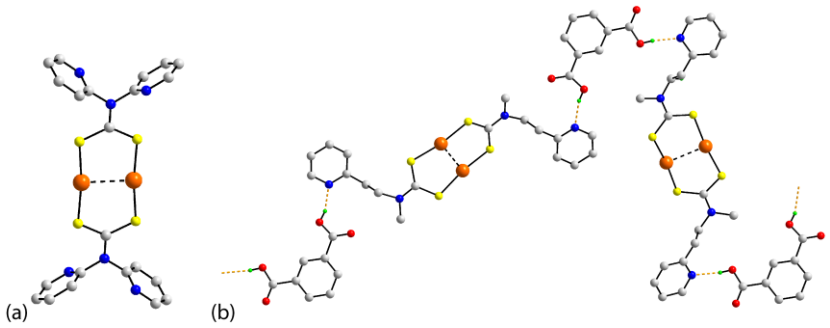

Figure 5. (**a**) Molecular structure for $[Au(L^7)]_2$ (**20**) and (**b**) supramolecular aggregation in the crystal of **21**, being a 1:1 co-crystal of $[Au(L^{12})]_2$ and isophthalic acid. Additional color code: oxygen, red. The orange dashed lines indicate hydroxyl-O–H···N(pyridyl) hydrogen bonds leading to a twisted supramolecular chain.

3.3. Structures of the Zinc-Triad Elements

The zinc-triad elements were the most populous in this survey, providing in excess of 40% of all structures covered herein. Of these, the least represented was zinc, having four examples only. Nevertheless, three distinct structural motifs were apparent. Crystals of homoleptic $[Zn(L^1)_2]_2$ (**22**) [35] and $[Zn(L^{13})_2]_2$ (**23**) [36] present di-nuclear molecules with that of **22**, shown in Figure 6a; an evaluation of solid-state luminescence was a motivation for the original studies. There were two quite distinct coordination modes for the dithiocarbamate ligand. One ligand was chelating [2.42 & 2.52 Å] while the other chelated one zinc atom [2.40 & 2.50 Å] and simultaneously linked a centrosymmetrically-related zinc atom via the pyridyl-nitrogen atom to form the di-nuclear aggregate of Figure 6a and a five-coordinate NS_4-donor set. This motif was readily related to the aggregate normally seen in the majority of homoleptic zinc bis(dithiocarbamate) structures [61], where one ligand was exclusively chelating with the other and at the same bridging, via one of the sulfur atoms, akin to that noted above for the bridging dithiocarbamate ligand in **17** (Figure 4a); in these circumstances a S_5 donor set was apparent. In this sense, the bridging pyridyl-nitrogen atom was simply substituted for the bridging-sulfur atom. However, this simple idea did not pertain to the remaining zinc dithiocarbamate structures to be described.

As illustrated in Figure 6b, a one-dimensional coordination polymer was noted in the crystal containing $[Zn(L^{14})_2]_n$. (**24**) [37]. It was noted that 4-methylpyridine was also present in the crystal of **24** (Table 1) but this did not coordinate zinc. The coordination modes of the dithiocarbamate ligands [chelating ligand: 2.40 & 2.50 Å and bridging: 2.35 & 2.67 Å] were as for each of **22** and **23**, but in this case, rather than dimer formation, an extended chain with a zig-zag topology was formed, owing to the formation of a Zn–N(pyridyl) bond. The common feature of **22**–**24** was the presence of a pyridyl-substituent on each dithiocarbamate ligand and the participation of only one of these in coordination with zinc. In the crystal of $[Zn(L^5)]_2$ (**25**) [36], the same situation applies and yet, a two-dimensional array ensued as each available pyridyl-nitrogen atom participated in coordination to symmetry-related zinc atoms.

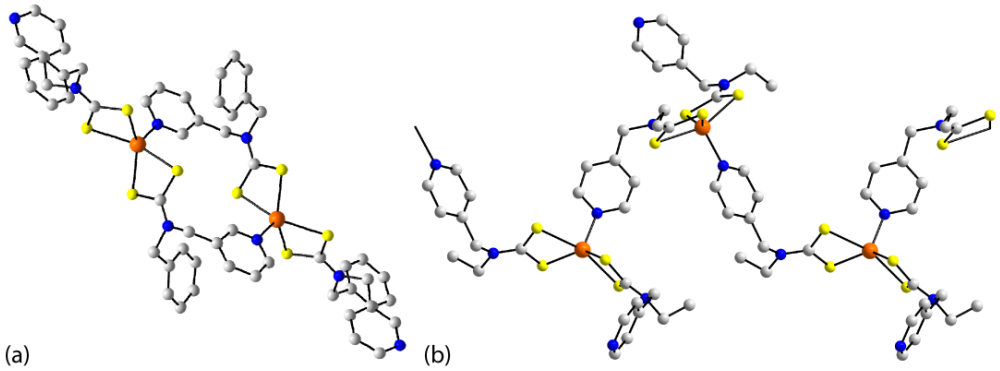

Figure 6. (**a**) The centrosymmetric, dimeric aggregate formed by $[Zn(L^{1})_2]_2$ in (**22**) and (**b**) supramolecular chain formed by $[Zn(L^{14})_2]_n$. in the crystal of **24**.

As shown in the lower view of Figure 7, each dithiocarbamate ligand of $[Zn(L^{5})]_2$ adopted a μ_2-bridging mode, employing the sulfur atoms to chelate one zinc atom [2.48 & 2.49 Å] and the pyridyl-nitrogen atom to link another; the zinc atom was located on a center of inversion. This resulted in an increase in the coordination number, as the zinc atom now existed within a trans-N_2S_4 donor set. The analogous structure to **25** but with the 3-pyridyl substituent, i.e., **23**, was a dimer. This being the case, it might be that steric congestion precluded further supramolecular aggregation. Clearly, systematic studies are highly desirable to resolve issues such as these but, of course, that depends on the availability of suitable crystalline materials, preferably solvent-free crystals grown under similar conditions of concentration, time, temperature, etc.

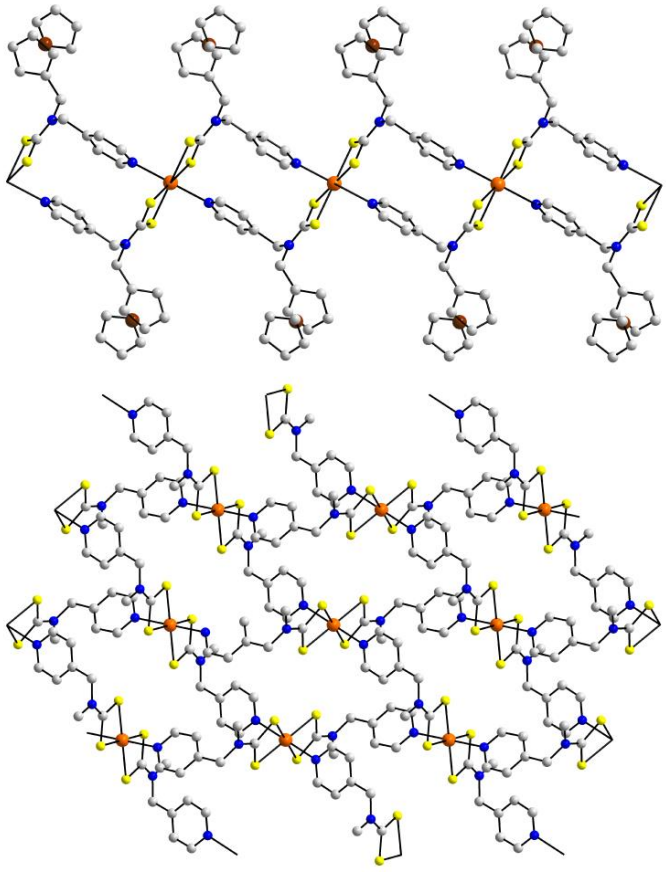

Figure 7. Two views of the two-dimensional array formed by $[Zn(L^{5})_2]_2$ in the crystal of **25**. In the lower view, only the α-carbon atom of the ferrocenyl (Fc) substituent is shown.

The first four cadmium(II) structures were zero-dimensional and the remaining were two-dimensional arrays of varying topologies. Three structures conformed to the general formula $Cd(L^x)_2(NN)$, namely x = 13, NN = 2,2′-bipyridyl (**26**) [38], and x = 13 (**27**) [38] and x = 14 (**28**) [36] for NN = 1,10-phenanthroline; **26** and **27** were noted for their ability to co-sensitize TiO_2 photoanodes, by virtue of the presence of ferrocenyl substituents [38]. The prototype for these structures (illustrated in Figure 8a) was **27**, which showed the cadmium atom to be chelated by two dithiocarbamate ligands [2.63 & 2.77 Å and 2.65 & 2.69 Å], as well as by the 1,10-phenanthroline molecule, to give a cis-N_2S_4 donor set. A di-nuclear molecule, akin to that found in each of **22** and **23**, was formed by $[Cd(L^{15})_2]_2$ in the crystal of **29** [39], as shown in Figure 8b. Here, an NS_4 donor set was manifested [Cd–S: 2.57 & 2.69 Å (chelating ligand) and 2.59 & 2.64 Å (bridging ligand)].

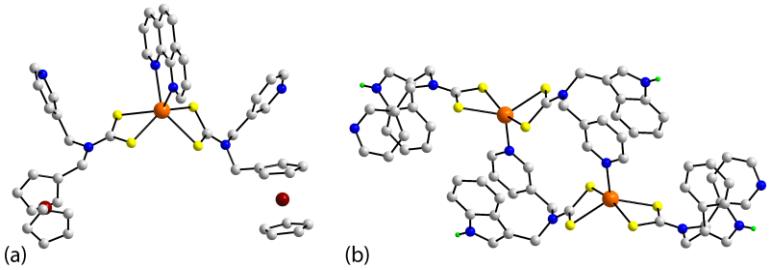

Figure 8. Molecular structures of (**a**) mononuclear $Cd(L^{13})_2$(1,10-phenanthroline) (**27**) and (**b**) di-nuclear and centrosymmetric $[Cd(L^{15})_2]_2$ in (**29**). Additional color code—hydrogen, green.

Of the six two-dimensional arrays formed by homoleptic cadmium dithiocarbamates, three distinct morphologies might be discerned. The first of these was found in the crystal of $[Cd(L^{14})_2]_n$ (**30**), which also contained non-coordinating 3-methylpyridine molecules [40]. Here, both pyridyl-nitrogen atoms of the dithiocarbamate ligand were involved in coordination, leading to cis-N_2S_4 donor sets, as the thiolate ends of the ligand were chelating [2.64 & 2.66 Å and 2.66 & 2.69 Å]. A plan view of the resulting two-dimensional array is shown in Figure 9, as well as a side-on view which highlighted the distinctive square-wave topology of the array; one plan view highlighted the formation of the coordination polyhedra.

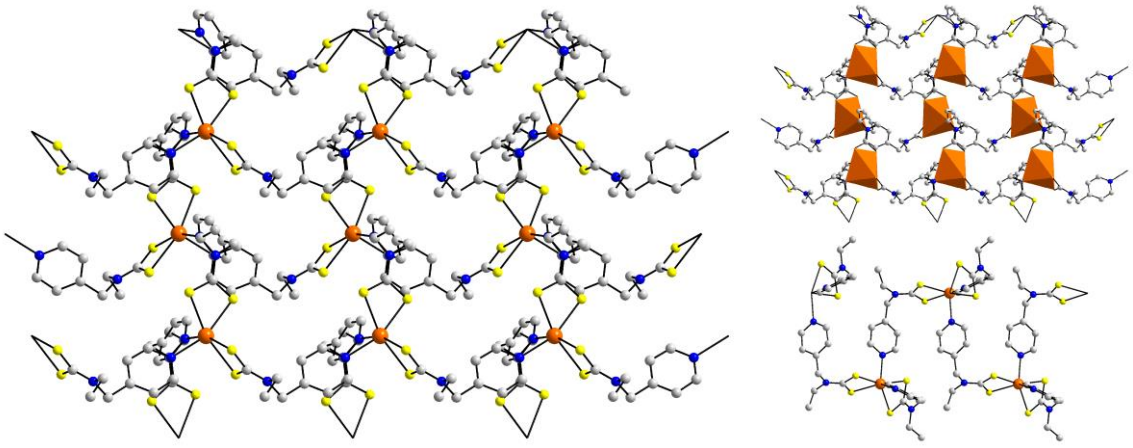

Figure 9. Plan and side-on views of the two-dimensional array in the crystals of $[Cd(L^{14})_2]_n$ (**30**); one of the plan views highlights the relative disposition of the cadmium atom coordination polyhedra.

Four structures, i.e., $[Cd(L^x)_2]_n$ for x = 1 (**31**), 11 (**32**) and 16 (**33**) [39], and x = 13 (**34**) [36] adopted a very similar structure in their crystals but, were not isostructural. As might be seen from Figure 10, showing images for **33**, the mode of coordination of the ligands was as for **30** [2 × 2.61 & 2.69 Å] but crucially resulted in trans-N_2S_4 donor sets; the cadmium atom in each of **33** and **34** lay on a center of inversion. The ensuing

arrangement was decidedly symmetric in appearance and from the side-on view, the array was undulating. When considered in terms of polyhedra alone, the packing resembled a hexagonal array.

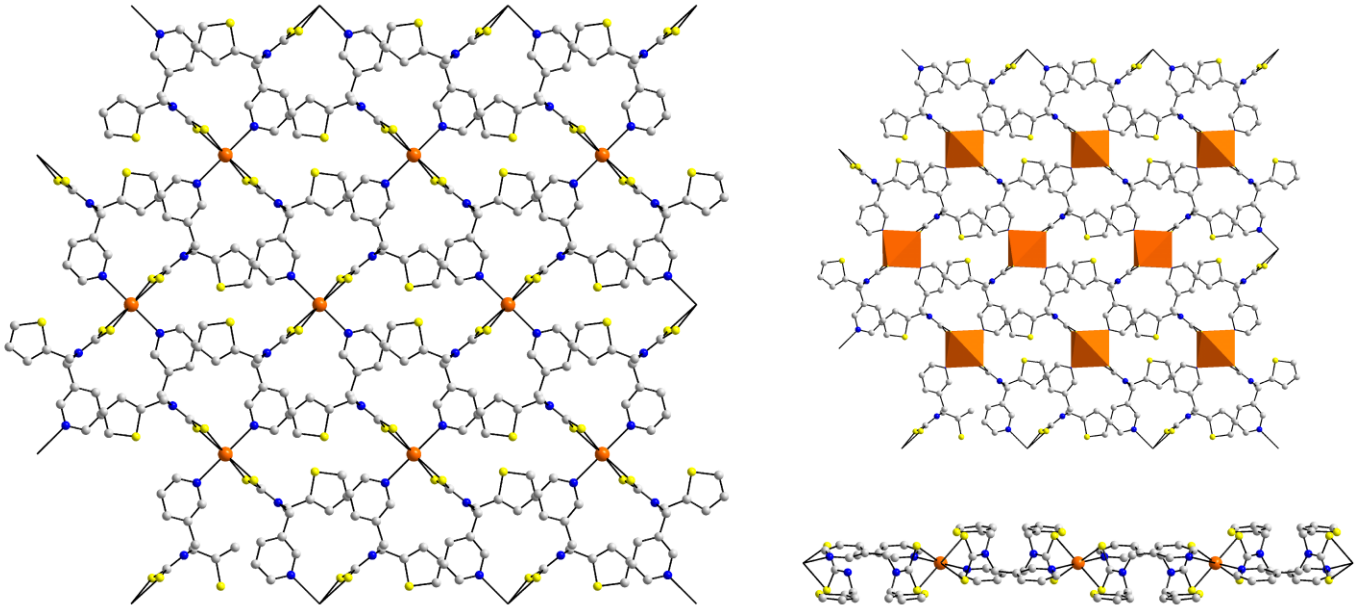

Figure 10. Plan and side-on views of the two-dimensional array in the crystals of $[Cd(L^{16})_2]_n$ (**33**); one plan view highlights the hexagonal pattern of the coordination polyhedra.

The sixth structure in this category was that of $[Cd(L^2)_2]_n$ (**35**) [39]. Again, the same features, i.e., coordination mode and trans-N_2S_4 donor sets, as noted above for **31**–**34**, were observed, but the relative disposition of the cadmium coordination geometries differed and the topology of the array was more jagged in appearance, Figure 11. The different arrangements of the coordination polyhedra in the three structural motifs noted for $[Cd(L^x)_2]_n$ is highlighted in Figures 9–11.

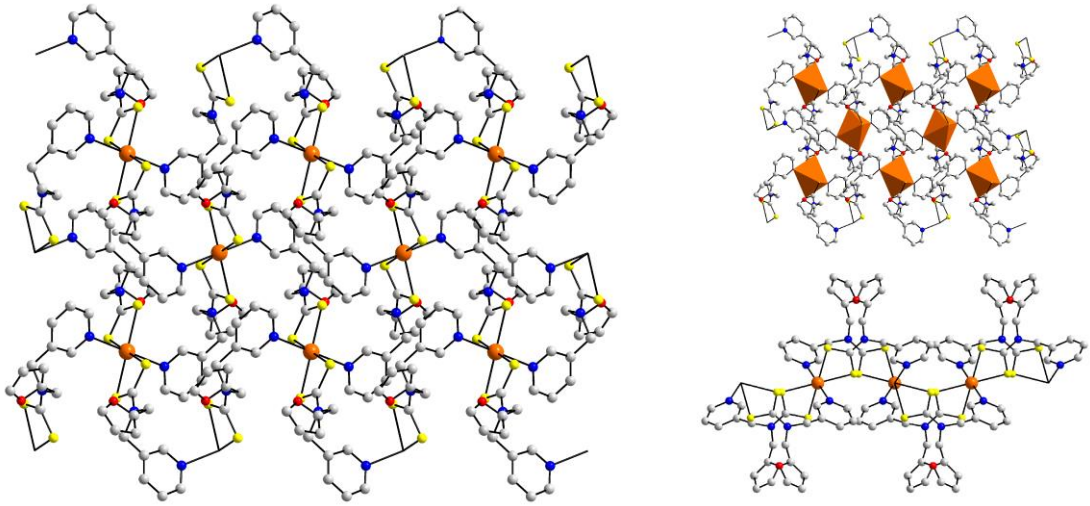

Figure 11. Plan and side-on views of the two-dimensional array in the crystals of $[Cd(L^2)_2]_n$ (**35**); one plan view highlights the arrangement of the coordination polyhedra.

Of all elements covered in the survey, mercury was the most prevalent, with 17 examples; organomercury structures were also present. Many studies were motivated by an evaluation of the influence of molecular packing upon luminescence characteristics.

Despite very similar formulae, quite distinct structural motifs were noted in many crystals. This was no better exemplified than by the six homoleptic mercury dithiocarbamates to be described. The common feature of $Hg(L^1)_2$ (**36**) [35] and $Hg(L^8)_2$ (**37**) [41] was a square–planar geometry for mercury, defined by two asymmetrically coordinating dithiocarbamate ligands, as shown for **36** in Figure 12a [2 × 2.40 & 2.95 Å]. Molecules assembled into a linear supramolecular chain via Hg···S interactions, therefore the mercury atom had a 4 + 2 coordination geometry. In each case, the mercury atom lay on a center of inversion and the Hg···S separations in the crystals leading to the linear chains were 3.22 and 3.21 Å, respectively. A distinct coordination geometry was found in each of $Hg(L^{17})_2$ (**38**) [42] and $Hg(L^{18})_2$ (**39**) [43], as shown for the former in Figure 12b. The tetrahedral S_4-donor set [2.45 to 2.64 Å] did not allow for further coordination by sulfur (or nitrogen) and so both molecules were monomeric in their crystals. The mercury atom in **39** lay on a 2-fold axis of symmetry. In $[Hg(L^{13})_2]_2$ (**40**), Figure 12c, molecules assembled about a center of inversion in the crystals to form a di-nuclear aggregate. The bidentate mode of coordination of one of the dithiocarbamate ligands in **40** was similar to that seen in several examples above, such as in the silver structure **17**, namely, asymmetrically chelating one mercury atom [2.44 & 3.12 Å] while simultaneously linking a centrosymmetric mate via one of the sulfur atoms [2.64 Å]. The other independent dithiocarbamate ligand was chelating only [2.44 & 2.83 Å]. A longer Hg···S bond of 3.12 Å was noted within the eight-membered $\{–HgSCS\}_2$ ring, which had a chair conformation. This Hg···S interaction might be considered a transannular contact and was shown as dashed bonds in Figure 12c. In the final homoleptic structure to be covered, i.e., $[Hg(L^{19})_2]_2$ (**41**) [42], a role for the pyridyl-nitrogen atom was apparent. As illustrated in Figure 12d, compared to **40**, the bridging dithiocarbamate ligand [2.50 & 2.72 Å] also employed the pyridyl-nitrogen atom, rather than a sulfur atom to connect the centrosymmetrically-related mercury center. The second dithiocarbamate ligand was asymmetrically chelating [2.42 & 3.00 Å] so the mercury atom existed within an NS_4-donor set. The result was a considerably larger, compared to **40**, central 16-membered $\{–HgSCNC_3N\}_2$ ring that was disposed about a center of inversion.

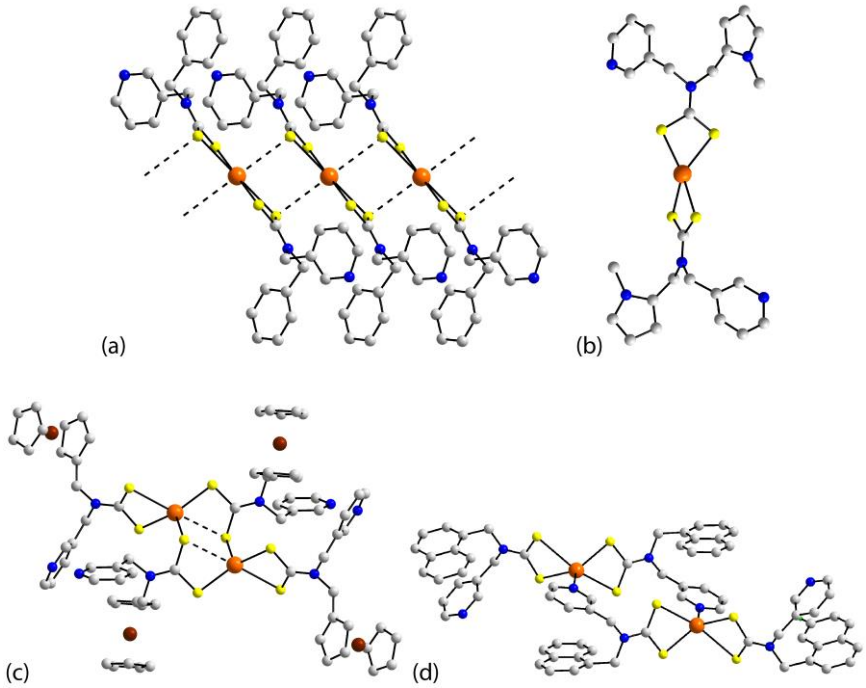

Figure 12. (**a**) The supramolecular chain in $Hg(L^1)_2$ (**36**) mediated by Hg···S interactions, (**b**) the tetrahedral molecule in $Hg(L^{17})_2$ (**38**), (**c**) the di-nuclear molecule in $[Hg(L^{13})_2]_2$ (**40**), and (**d**) the di-nuclear molecule in $[Hg(L^{19})_2]_2$ (**41**).

There were five phenylmercury(II) dithiocarbamates and these adopted two distinct motifs depending on the mode of coordination of the dithiocarbamate ligand. The first motif was found in $[PhHg(L^x)]_2$ for x = 5 (**42**) [44], x = 17 (**43**) [42] and x = 20 (**44**) [35]. This motif is illustrated for **43** in Figure 13a. Here, the mercury atom was asymmetrically coordinated by the dithiocarbamate ligand [2.39 & 2.89 Å] and the centrosymmetrically-related molecules were linked via the Hg···S interactions of 3.14 Å; the equivalent separations in **42** and **44** were 3.18 and 3.19 Å, respectively. The $\{–HgSCS\}_2$ ring had a chair conformation with the dithiocarbamate ligands lying either side of the central $\{\cdots HgS\}_2$ core. The second motif, adopted by $[PhHg(L^{18})]_2$ (**45**) [43] and $PhHg(L^{21})]_2$ (**46**) [41], illustrated for **45** in Figure 13b, also featured asymmetrically chelating dithiocarbamate ligands [2.38 & 3.02 Å] but the connections between centrosymmetrically-related mates were via the Hg–N bonds. Thus, there was a transformation from one motif to another, as the position of the pyridyl-nitrogen atom migrated from the 3-position in **43** to the 4-position in **45**. This might indicate a steric influence in directing the mode of coordination coming into play but it was noted that **44** also carried a 4-pyridyl substituent. Then again, in the crystal of **44**, there was occluded methanol and this formed a methanol-O–H···N(pyridyl) hydrogen bond, already noted as a reliable supramolecular synthon [59].

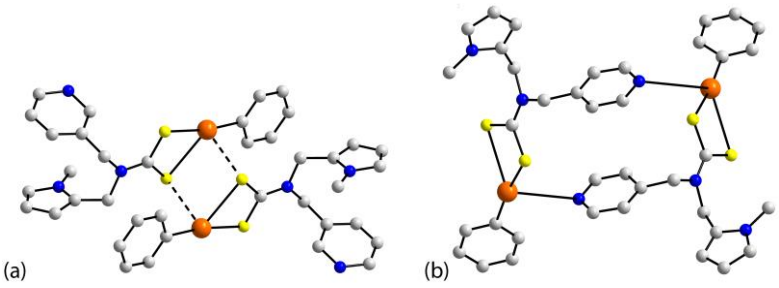

Figure 13. (**a**) The supramolecular dimer in $[PhHg(L^{17})]_2$ (**43**) mediated by the Hg···S interactions and (**b**) the di-nuclear molecule in $[PhHg(L^{18})]_2$ (**45**).

The next four molecules assembled into supramolecular chains in their crystals. All four resultant topologies were distinct. In $[Hg(L^{10})_2]_n$ (**47**) [43], both dithiocarbamate ligands were bidentate, bridging two mercury centers to form eight-membered $\{–HgSCS\}_2$ rings with a chair conformation; the bridges were non-symmetric [2 × 2.39 & 2.95 Å]. Within each ring, there were two transannular Hg···S interactions [2 × 3.05 Å] such that one of the dithiocarbamate ligands might be considered tri-connective. The rings were concatenated into a chain, sharing mercury atoms at the corners. The one-dimensional chain was propagated by glide-symmetry with the mercury atoms lying on 2-fold axes of symmetry, perpendicular to the axis of the chain. Side- and end-on views of the chain are shown in Figure 14a. A variation was noted in the crystal of $[Hg(L^{22})_2]_n$ (**48**) [35]; two independent molecules comprised the asymmetric-unit. The mercury atom in each independent molecule was chelated by two asymmetrically coordinating dithiocarbamate ligands [2.41 & 3.01 Å and 2.42 & 3.01 Å for molecule 1 and 2.43 & 2.83 and 2.42 & 3.00 Å for molecule 2], with the sulfur atom forming the longer of the Hg–S bonds bridging to a second mercury atom [2.92 and 2.90 Å, respectively]. The chain was propagated by translational symmetry but owing to the relative disposition of the two molecules in the asymmetric-unit, the chain had a zig-zag topology, as seen in the two views of Figure 14b. While the bridges leading to the chains in **47** and **48** involved sulfur atoms, in the next two crystals, it was the participation of the pyridyl-nitrogen atom that led to the formation of the chains.

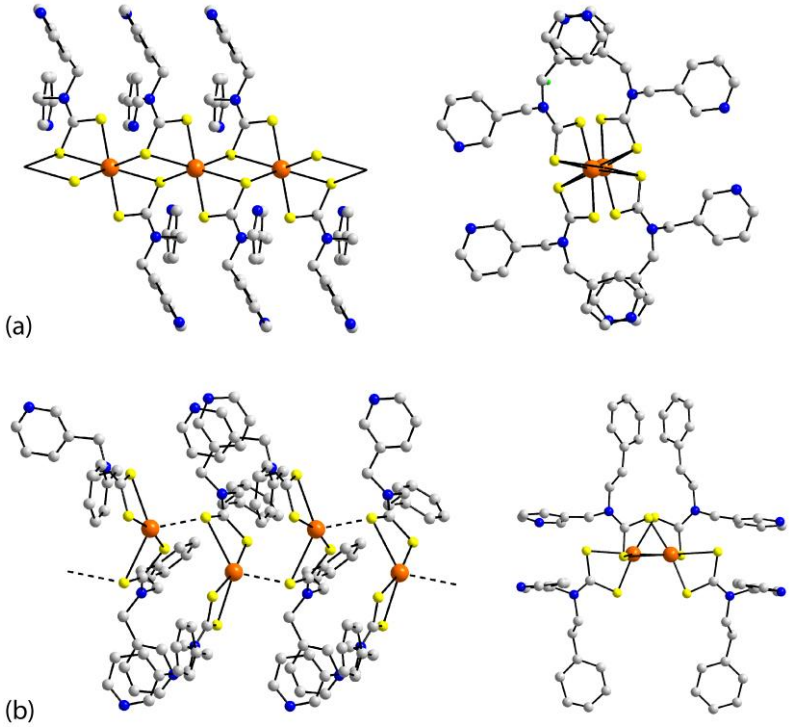

Figure 14. The zig-zag supramolecular chain mediated by the Hg···S interactions in (**a**) $[Hg(L^{10})_2]_n$ (**47**) and (**b**) $[Hg(L^{22})_2]_n$ (**48**).

Two distinct structural motifs were observed in the crystals of $[Hg(L^{21})_2]_n$ (**49**) and $[Hg(L^{23})_2]_n$ (**50**) [35]. In the former, the mercury atom was chelated by two dithiocarbamate ligands, one forming close to symmetric Hg–S bonds [2.60 & 2.66 Å], with the other coordinating less symmetrically [2.51 & 2.84 Å]. The fifth site about the mercury atom was occupied by a pyridyl-nitrogen atom from a translationally-related molecule, giving rise to a NS_4-donor-set and a one-dimensional chain with a linear topology, Figure 15a. In **50**, Figure 15b, a similar mode of coordination of the dithiocarbamate ligands was noted, whereby the mercury atom was coordinated by two dithiocarbamate ligands, one forming almost symmetric Hg–S bonds [2.51 & 2.66 Å] and the other forming quite asymmetric Hg–S bonds [2.39 & 3.11 Å]. The coordination was completed by a pyridyl-nitrogen atom derived from a symmetry related molecule to define a NS_4-donor set, and a supramolecular chain with a zig-zag (glide-symmetry) topology.

One of the homoleptic mercury dithiocarbamates assembled into a two-dimensional array in the crystal, i.e., $[Hg(L^9)_2]_n$ (**51**) [35]. Different views of the assembly are shown in Figure 16. The mercury atom lay on a center of inversion and was coordinated by the dithiocarbamate ligand in an asymmetric mode [2.48 & 2.82 Å]. The distorted N_2S_4-donor set was completed by two pyridyl-nitrogen atoms derived from two symmetry-related dithiocarbamate ligands, as a result, an array was formed with a flat topology. The alignment of successive rows of the polyhedra was off-set.

The final structure to be described among the zinc-triad elements is a phenylmercury derivative, $[PhHg(L^8)]_n$ (**52**) [41]. As usual for the phenylmercury dithiocarbamates, the dithiocarbamate ligands formed short and long Hg–S interactions [2.41 & 2.99 Å]. The weakly bound sulfur atom formed a bridge [3.20 Å] to a symmetry-related mercury atom to form a helical chain. The chains were connected into a layer via pyridyl-nitrogen bridges to translationally-related molecules, resulting in the undulating assembly shown in Figure 17. This arrangement highlighted the cooperativity between bridging dithiocarbamate-sulfur and pyridyl-nitrogen atoms.

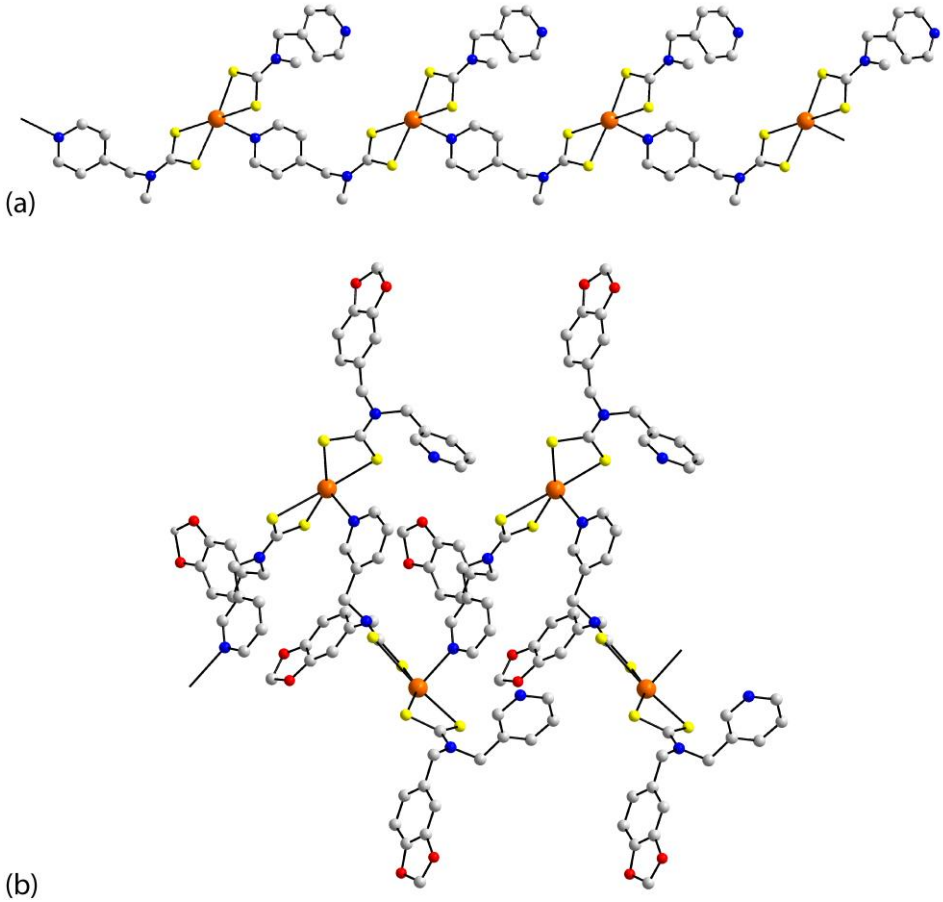

Figure 15. The supramolecular chain mediated by the Hg···S interactions in (**a**) linear $[Hg(L^{21})_2]_n$ (**49**) and (**b**) zig-zag $[Hg(L^{23})_2]_n$ (**50**).

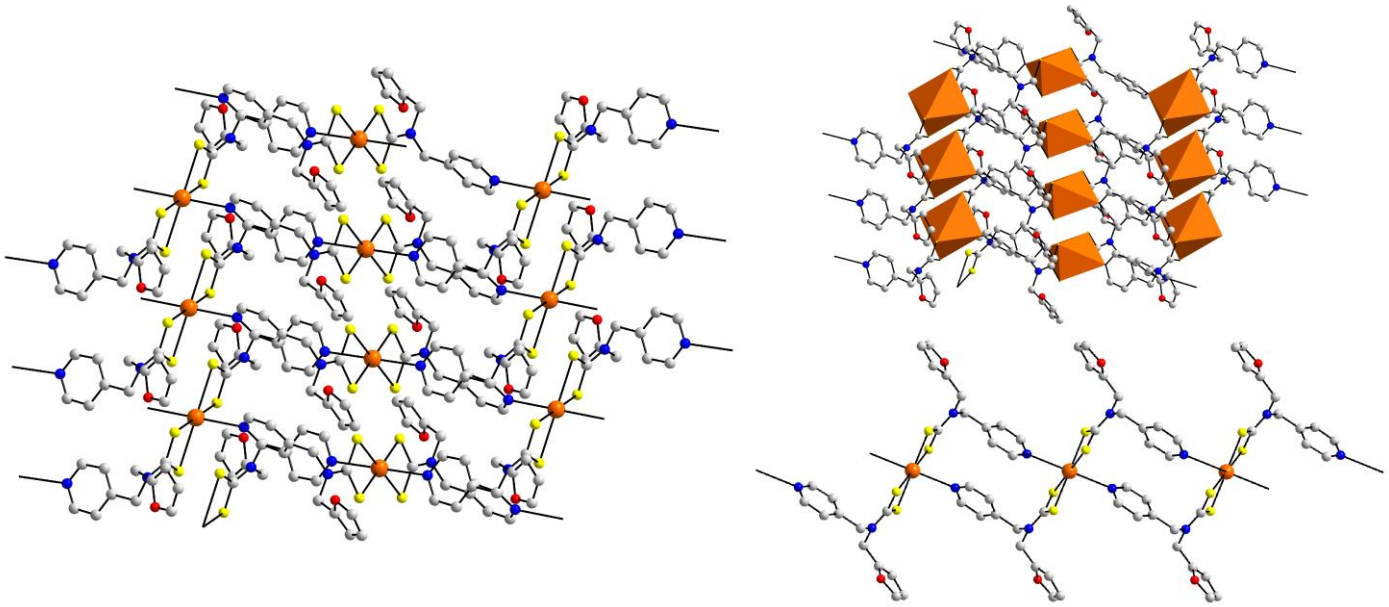

Figure 16. Views of the two-dimensional array in the crystal of $[Hg(L^{9})_2]_n$ (**51**); one plan view highlights the arrangement of the coordination polyhedra.

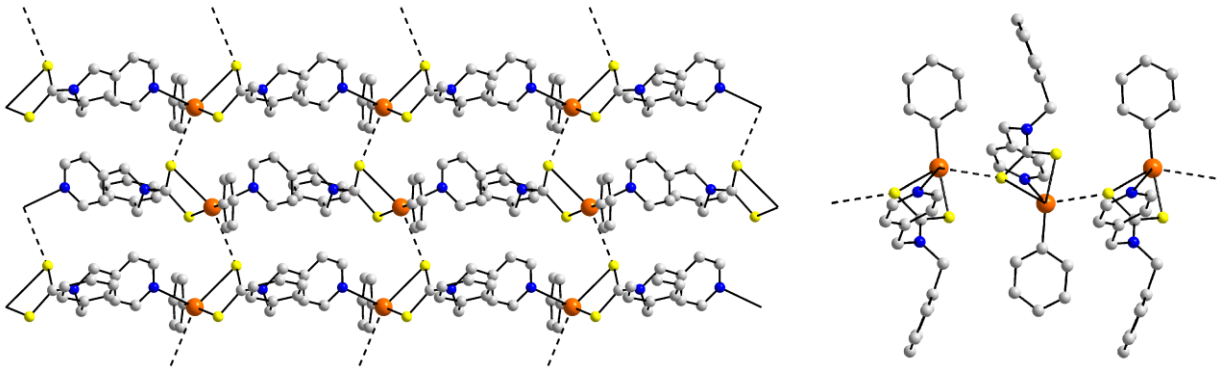

Figure 17. Views of the two-dimensional array in the crystal of $[PhHg(L^{8})]_{n}$ (**52**).

3.4. Structures of Thallium(I)

The eight structures of thallium(I) were homoleptic and conformed to the general formula $[Tl(L^{x})]_{n}$, with all crystals being solvent-free. Two basic structural motifs were observed. The first of these was adopted by a single example only, namely $[Tl(L^{24})]_{n}$ (**53**) [45]. As illustrated from the views in Figure 18, the thallium(I) center was chelated by a dithiocarbamate ligand in a symmetric mode [2.97 & 3.04 Å for the first independent molecule and 2.96 & 3.08 Å for the second]. Each independent molecule self-associated about a center of inversion via two additional Tl···S interactions [3.06 & 3.30 Å for the first dimer and 3.10 & 3.11 Å for the second dimer]. The sulfur atom forming the longer of the specified Tl···S interactions provided a bridge to the second independent dimer [3.41 Å] and in this sense the first dithiocarbamate ligand was penta-connective, whereas the second ligand was tetra-connective. The pairs of dimeric units were connected into a chain via translational symmetry so the resulting topology was somewhat flattened. By contrast to **53**, the seven remaining structures adopted a very similar, two-dimensional structural motif.

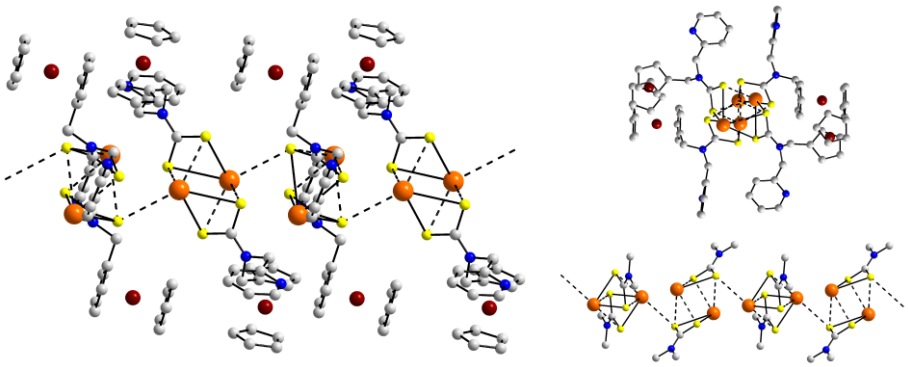

Figure 18. Views of the one-dimensional chain in the crystal of $[Tl(L^{24})]_{n}$ (**53**).

The second structural motif adopted for $[Tl(L^{x})]_{n}$ was found for x = 1 (**54**), x = 11 (**55**), x = 13 (**56**), x = 23 (**57**) [46], x = 16 (**58**), x =25 (**59**) and x = 26 (**60**) [45]. Indeed, structures **54**, **55**, **56**, and **58** were isostructural, as were the trio of structures **57**, **59**, and **60**. The differentiation between the supramolecular assembly of **53**, as compared with **54**–**60**, was the participation of pyridyl-nitrogen atoms, in coordination, in the latter series. This had a crucial result that two-dimensional arrays eventuated. The exemplar structure was that of **54**. Here, the thallium(I) center was chelated in a symmetric mode by a dithiocarbamate ligand [2.96 & 3.05 Å], which linked to a centrosymmetrically-related thallium via two additional Tl···S contacts [3.22 & 3.33 Å] to form a dimeric aggregate, akin to that seen in **53**. Each thallium(I) atom formed an additional Tl···S contact that extended laterally [3.50 Å]. Importantly, the pyridyl-nitrogen atom also connected to thallium, ensuring the stability of the two-dimensional array that had an undulating topology. Alternatively, the

structure might be described more simply in terms of the chelating dithiocarbamate ligand linked to neighbors via the pyridyl-nitrogen atom, as shown in the top right-hand view of Figure 19. This chain had a distinctive, square-wave topology, and was connected to the array via the aforementioned, second tier Tl···S interactions.

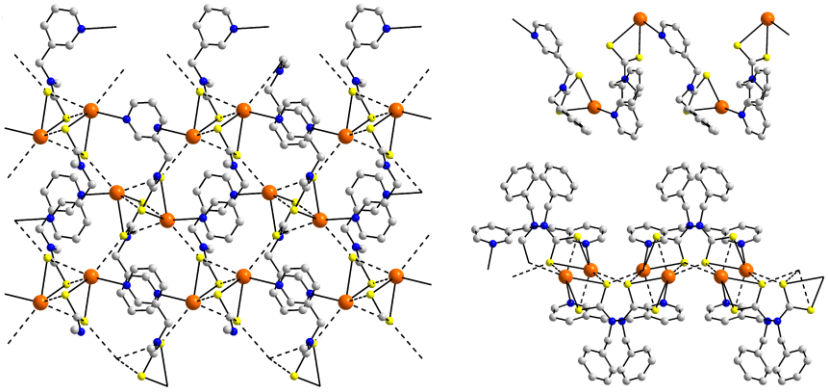

Figure 19. Views of the two-dimensional array in the crystal of $[Tl(L^1)]_n$ (**54**).

3.5. Structures of Organotin(IV)

The nine organotin structures might be conveniently divided into two groups, with the majority not having tin interacting with a pyridyl-nitrogen atom. Three distinct structural motifs were noted among the first five organotin structures and these conformed with literature expectation [62], with the first three examples featuring skew-trapezoidal bipyramidal geometries for tin, i.e., in $(nBu)_2Sn(L^8)_2$ (**61**) [47], $(nBu)_2Sn(L^{14})_2$ (**62**) [48], and $Ph_2Sn(L^{14})_2$ (**64**) [48]. This is illustrated for **62** in Figure 20a. The tin atom, lying on a 2-fold axis of symmetry, was asymmetrically chelated by two dithiocarbamate ligands [2.52 & 3.01 Å], which define a trapezoidal plane. The organic substituents lay over the weaker Sn···S bonds to complete the C_2S_4-donor set; each of **61** and **64** also manifested a 2-fold symmetry. A recent survey [63] reported that diphenyltin dithiocarbamates adopted such geometries in about one-third of their structures, with the majority being based on cis-C_2S_4 donor sets with a more symmetric mode of coordination for the dithiocarbamate ligand. This is exemplified in Figure 20b for $Ph_2Sn(L^1)_2$ (**63**) [47], which is 2-fold symmetric and has intermediate Sn–S bond lengths [2.59 & 2.68 Å]. The triphenyltin derivative, $Ph_3Sn(L^{27})$ (**65**) [49], Figure 20c, also conformed to expectation with the dithiocarbamate ligand coordinating in an asymmetric mode [2.46 & 3.06 Å].

A rather unusual multi-functional ligand was evident in L^{28}. Here, there were two dithiocarbamate residues connected in the 2,5-positions of a pyridyl ring that gave rise to a di-anion with multiple coordination sites. In $(Ph_3Sn)_2(L^{28})$ (**66**) [49], each dithiocarbamate ligand asymmetrically chelated a tin atom [2.45 & 3.11 Å and 2.46 & 3.11 Å; the molecule lacked symmetry] resembling the coordination mode in the mono-nuclear species **65**. This mode of coordination gave rise to a di-nuclear molecule with an open configuration, as shown in Figure 20d. When the diorganotin centers were introduced in place of the triorganotin species, a cyclic dimer was noted in the crystal of $[(PhCH_2)_2Sn)(L^{28})]_2$ (**67**) [49], as illustrated in Figure 20e. The coordination geometries for the tin atoms (the molecule lacks symmetry) is as described for **61**, **62**, and **64** above. The Sn–S bonds [2.50 & 2.96 Å and 2.54 & 3.03 Å] for one molecule closely followed that indicated for **62** but, a difference was noted for the second independent tin atom where one ligand coordinated in the expected mode [2.51 & 2.83 Å] but the other was decidedly more asymmetric [2.54 & 3.29 Å]. As for the previous organotin dithiocarbamates, no role in coordination was noted for the pyridyl-nitrogen atom. The two remaining structures were rather exceptional.

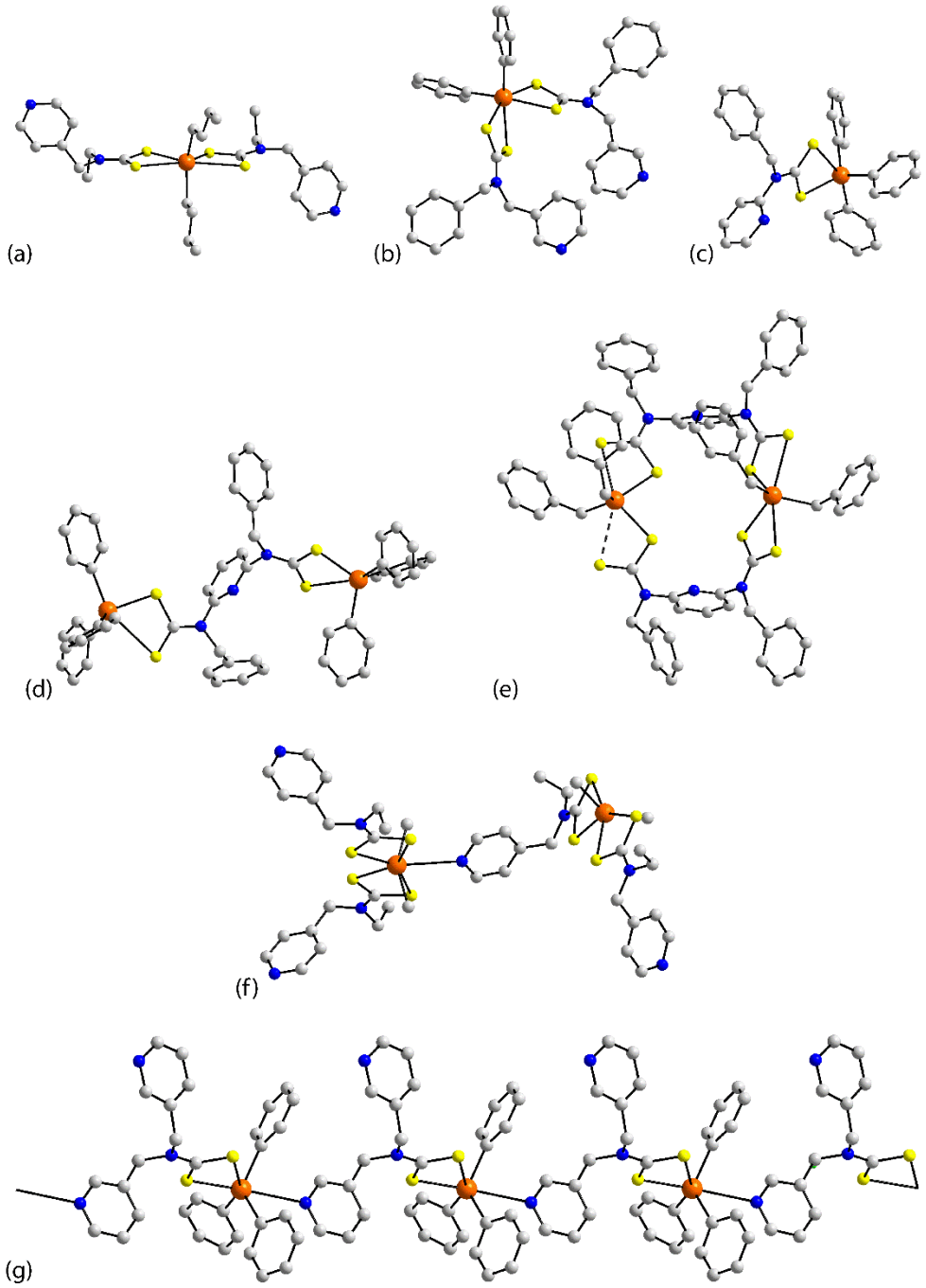

Figure 20. Molecular structures of (**a**) $(nBu)_2Sn(L^{14})_2$ (**62**), (**b**) $Ph_2Sn(L^1)_2$ (**63**) and (**c**) $Ph_3Sn(L^{27})$ (**65**), (**d**) the open dimer in $(Ph_3Sn)_2(L^{28})$ (**66**), (**e**) the cyclic dimer in the crystal of $[(PhCH_2)_2Sn)(L^{28})]_2$ (**67**), (**f**) the dimer in the crystal of $[Me_2Sn(L^{14})_2]_2$ (**68**), and (**g**) the one-dimensional chain in $[Ph_3Sn(L^{11})]_n$ (**69**).

The crystallographic asymmetric-unit of $[Me_2Sn(L^{14})_2]_2$ (**68**) [48] comprised two independent molecules. As illustrated in Figure 20f, one molecule adopted the expected skew-trapezoidal pyramidal geometry and this donated one of the pyridyl-nitrogen atoms to the second molecule to form a dimer. The expanded coordination geometry for the second molecule was based on a pentagonal bipyramidal geometry, as the incoming nitrogen atom occupied a position between the less strongly bound sulfur atoms. It is of interest to comment on the systematic changes in geometric parameters. Thus, there was an expansion of the Sn–S bond lengths from the low-coordinate species [2.54 & 2.94 Å and 2.55 & 2.91 Å] to the high-coordinate species [2.58 & 2.94 Å and 2.61 & 3.00 Å], and an

expansion of the C–Sn–C angle [143° cf. 153°]. Two independent molecules also comprised the asymmetric-unit of $[Ph_3Sn(L^{11})]_n$ (**69**) [47]. These also behaved differently, emphasizing the enigmatic behavior in these systems. While one molecule adopted the anticipated geometry, as noted for **67**, the other formed additional Sn–N interactions to generate the linear chain shown in Figure 20g. The Sn–S bond lengths in the first independent molecule [2.47 & 3.04 Å] were shorter than those for the tin atom in the chain [2.52 & 3.22 Å], reflecting the increased coordination number within the C_3NS_2-donor set, which defined a skew-trapezoidal bipyramidal geometry with the phenyl groups lying over the longer Sn–S and Sn–N bonds.

3.6. Structures of Bismuth(III)

The final group of structures could also be divided, depending on the mode of supramolecular association. Well known for their anti-cancer potential [64], interest in these compounds largely related to their biological activity. Additionally, the propensity of the homoleptic bismuth dithiocarbamates to aggregate into supramolecular spheres via Bi···S interactions [65] is well-documented, reflecting the thiophilic nature of bismuth. This was the case for the first three examples, namely, $[Bi(L^6)_3]_2$ (**70**) [50], $[Bi(L^{25})_3]_2$ (**71**), and $[Bi(L^{28})_3]_2$ (**72**) [51]. In **70**, Figure 21a, the bismuth center was coordinated by three dithiocarbamate ligand [2.70 to 3.22 Å], and centrosymmetrically-related molecules assembled to form a dimer via a pair of Bi···S contacts [3.17 Å]. A similar situation pertained for **71** [2.67 to 3.12 Å], Figure 21b, but, there were four intra-dimer Bi···S contacts [2 × 3.09 to 3.14 Å] to stabilize the dimer. Simply changing the remote substituent from a chloride in **71** to a bromide, giving $[Bi(L^{29})_3]_n$ (**73**) [51], resulted in a profound change in supramolecular aggregation.

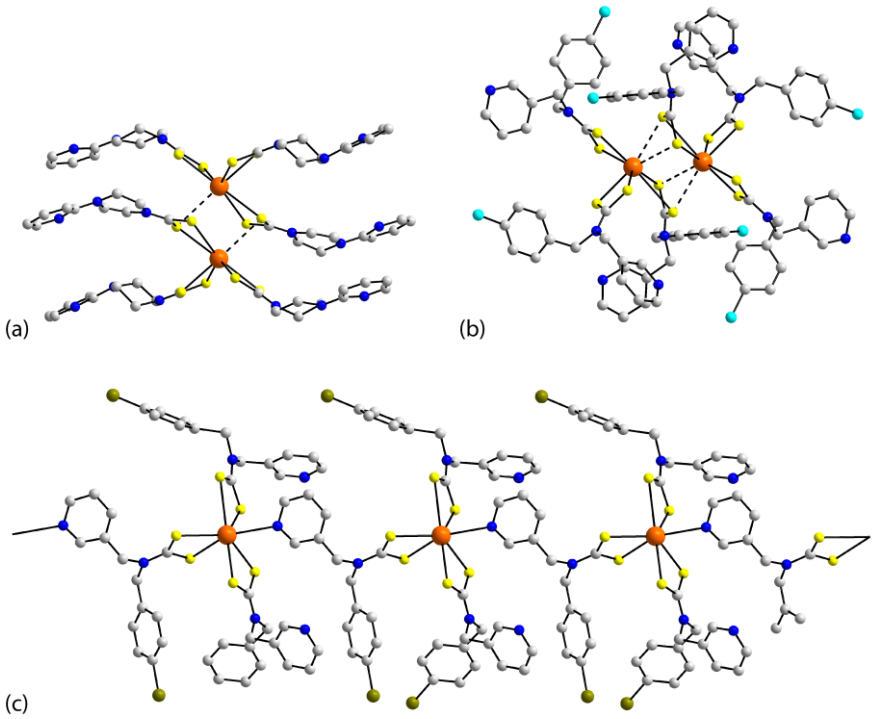

Figure 21. Supramolecular aggregation in the crystals of (**a**) $[Bi(L^6)_3]_2$ (**70**) and (**b**) $[Bi(L^{25})_3]_2$ (**71**), via Bi···S interactions, and (**c**) $[Bi(L^{29})_3]_n$ (**73**) via Bi–N interactions. Additional color code—bromide, dark-green.

As seen from Figure 21c, there were three chelating dithiocarbamate ligands [2.67 to 3.04 Å] and one of the dithiocarbamate ligands also connected to a translationally-related molecule via the pyridyl-nitrogen atom to generate a linear, one-dimensional arrangement. The resultant NS_6-donor was a based on a pentagonal-bipyramidal geometry, with the nitrogen and one sulfur atom occupying the axial positions.

4. Discussion

Among the ubiquitous dithiocarbamate ligands, those carrying pyridyl functionality only formed a small subset. There were 30 different pyridyl-functionalized dithiocarbamate ligands that were characterized in 73 crystal structures. Indeed, crystal structures were only reported for the nickel-, copper-, and zinc-triad elements, along with examples of thallium(I), organotin(IV), and bismuth(III) structures. Approaching half the structures were derived from the zinc-triad elements with a high representation of mercury, including organomercury, structures. The involvement of the pyridyl-nitrogen atom(s) often led to the formation of dimeric aggregates but also one-dimensional chains and two-dimensional arrays. The limited study of these ligands, thus far, clearly indicates there is enormous scope to expand this chemistry, especially that of the main group elements.

Generally, the transition metal structures did not see a role for nitrogen in coordinating the metal center, with the individual structures resembling their non-pyridyl-functionalized congeners. The situation was rather different for the reported main group element structures where participation of the pyridyl-nitrogen atom was often observed to give rise to quite distinct and previously unknown structural motifs and disparate coordination geometries. The coordination of pyridyl-nitrogen notwithstanding, many molecules assembled via M$\cdots$S secondary bonding interactions [66] rather than M–N dative bonding. More perplexing was the problematic formation of the M$\cdots$S secondary bonding versus the M–N dative bonding. These interactions also worked in concert, i.e., cooperated, to form higher dimensional architectures. Additionally, it was noted that a seemingly small change in a non-participating substituent could result in a very different structural motif. The most perplexing observation was the different behavior exhibited by the independent molecules comprising the asymmetric-unit within a crystal, for example, for $[Me_2Sn(L^{14})_2]_2$ (**68**) [48] and $[Ph_3Sn(L^{11})]_n$ (**69**) [47]. This being stated, it is well-established that dithiocarbamate structural chemistry, as revealed by X-ray crystallographic studies, can be quite unpredictable [52,61,62,65,67–69]. This present analysis of the structural chemistry of pyridyl-functionalized dithiocarbamate ligands vindicated this conclusion and clearly added to the rich tapestry of structures found for dithiocarbamate ligands.

5. Conclusions

The structural chemistry of pyridyl-functionalized dithiocarbamate ligands is relatively unexplored and given the unpredictable behavior exhibited thus far, competition between the formation of M–N dative bonds and M$\cdots$S secondary bonding interactions, and the appearance of unprecedented structural motifs, further examination of these ligands is clearly warranted. Especially, systematic studies under controlled crystallization conditions are needed.

Funding: This research was funded by Sunway University Sdn Bhd, grant number GRTIN-IRG-01-2021.

Institutional Review Board Statement: Not applicable.

Informed Consent Statement: Not applicable.

Data Availability Statement: All data are included in the review article.

Conflicts of Interest: The author declares no conflict of interest.

References

1. Debus, H. Ueber die Verbindungen der Sulfocarbaminsäure. *Justus Liebigs Ann. Chem.* **1850**, *73*, 26–34. [CrossRef]
2. Delépine, M. Metallic salts of dithiocarbamic acids; preparation of isothiocyanates in the aliphatic series. *Compt. Rend.* **1907**, *144*, 1125–1127.
3. Coucouvanis, D. The chemistry of the dithioacid and 1,1-dithiolate complexes. In *Progress in Inorganic Chemistry*; Lippard, S.J., Ed.; John Wiley & Sons: Hoboken, NJ, USA, 1970; Volume 11, pp. 234–371. [CrossRef]
4. Eisenberg, R. Structural systematics of 1,1- and 1,2-dithiolato chelates. In *Progress in Inorganic Chemistry*; Lippard, S.J., Ed.; John Wiley & Sons: Hoboken, NJ, USA, 1970; Volume 12, pp. 295–369. [CrossRef]

5. Coucouvanis, D. The chemistry of the dithioacid and 1,1-dithiolate complexes, 1968–1977. In *Progress in Inorganic Chemistry*; Lippard, S.J., Ed.; John Wiley & Sons: Hoboken, NJ, USA, 1979; Volume 26, pp. 301–469. [CrossRef]
6. Hogarth, G. Transition metal dithiocarbamates: 1978–2003. In *Progress in Inorganic Chemistry*; Karlin, K.D., Ed.; John Wiley & Sons: Hoboken, NJ, USA, 2005; Volume 53, pp. 71–561. [CrossRef]
7. Heard, P.J. Main group dithiocarbamate complexes. In *Progress in Inorganic Chemistry*; Karlin, K.D., Ed.; John Wiley & Sons: Hoboken, NJ, USA, 2005; Volume 53, pp. 1–69. [CrossRef]
8. Lee, S.M.; Heard, P.J.; Tiekink, E.R.T. Molecular and supramolecular chemistry of mono- and di-selenium analogues of metal dithiocarbamates. *Coord. Chem. Rev.* **2018**, *375*, 410–423. [CrossRef]
9. Poplaukhin, P.; Tiekink, E.R.T. (μ-Piperazine-1,4-dicarbodithioato-κ^4S,S′:S″,S‴)bis[triphenyltin(IV)] dichloromethane solvate. *Acta Crystallogr. Sect. E Crystallogr. Commun.* **2008**, *64*, m1177. [CrossRef] [PubMed]
10. Lee, S.M.; Tiekink, E.R.T. A structural survey of poly-functional dithiocarbamate ligands and the aggregation patterns they sustain. *Inorganics* **2021**, *9*, 7. [CrossRef]
11. Yu, S.-Y.; Sun, Q.-F.; Lee, T.K.-M.; Cheng, E.C.-C.; Li, Y.-Z.; Yam, V.W.-W. Au_{36} crown: A macrocyclization directed by metal-metal bonding interactions. *Angew. Chem. Int. Ed.* **2008**, *47*, 4551–4554. [CrossRef] [PubMed]
12. Wang, S.; Xu, J.; Wang, J.; Wang, K.-Y.; Dang, S.; Song, S.; Liu, D.; Wang, C. Luminescence of samarium(III) bis-dithiocarbamate frameworks: Codoped lanthanide emitters that cover visible and near-infrared domains. *J. Mater. Chem. C* **2017**, *5*, 6620–6628. [CrossRef]
13. Castillo, M.; Criado, J.J.; Macias, B.; Vaquero, M.V. Chemistry of dithiocarbamate derivatives of amino acids. I. Study of some dithiocarbamate derivatives of linear α-amino acids and their nickel(II) complexes. *Inorg. Chim. Acta* **1986**, *124*, 127–132. [CrossRef]
14. Liebing, P.; Witzorke, J.; Oehler, F.; Schmeide, M. Dithiocarbamatocarboxylate (DTCC) ligands—building blocks for hard/soft-heterobimetallic coordination polymers. *Inorg. Chem.* **2020**, *59*, 2825–2832. [CrossRef]
15. Taylor, R.; Wood, P.A. A million crystal structures: The whole is greater than the sum of its parts. *Chem. Rev.* **2019**, *119*, 9427–9477. [CrossRef]
16. Bruno, I.J.; Cole, J.C.; Edgington, P.R.; Kessler, M.; Macrae, C.F.; McCabe, P.; Pearson, J.; Taylor, R. New software for searching the Cambridge Structural Database and visualizing crystal structures. *Acta Crystallogr. Sect. B Struct. Sci. Cryst. Eng. Mater.* **2002**, *58*, 389–397. [CrossRef]
17. Brandenburg, K.; Berndt, M. *DIAMOND, Version 3.2k*; GbR: Bonn, Germany, 2006.
18. Rajput, G.; Singh, V.; Gupta, A.N.; Yadav, M.K.; Kumar, V.; Singh, S.K.; Prasad, A.; Drew, M.G.B.; Singh, N. Unusual C–H···Ni anagostic interactions in new homoleptic Ni(II) dithio complexes. *CrystEngComm* **2013**, *15*, 4676–4683. [CrossRef]
19. Halimehjani, A.Z.; Torabi, S.; Amani, V.; Notash, B.; Saidi, M.R. Synthesis and characterization of metal dithiocarbamate derivatives of 3-((pyridin-2-yl)methylamino)propanenitrile: Crystal structure of [3-((pyridin-2-yl)methylamino)propanenitrile dithiocarbamato] nickel(II). *Polyhedron* **2015**, *102*, 643–648. [CrossRef]
20. Yadav, M.K.; Rajput, G.; Prasad, L.B.; Drew, M.G.B.; Singh, N. Rare intermolecular M···H–C anagostic interactions in homoleptic Ni(II)–Pd(II) dithiocarbamate complexes. *Polyhedron* **2015**, *39*, 5493–5499. [CrossRef]
21. Kumar, V.; Singh, V.; Gupta, A.N.; Singh, S.K.; Drew, M.G.B.; Singh, N. Cooperative influence of ligand frameworks in sustaining supramolecular architectures of Ni(II)/Pd(II) heteroleptic dithio-dipyrrin complexes via non-covalent interactions. *Polyhedron* **2015**, *89*, 304–312. [CrossRef]
22. Gupta, A.N.; Kumar, V.; Singh, V.; Manar, K.K.; Drew, M.G.B.; Singh, N. Intermolecular anagostic interactions in group 10 metal dithiocarbamates. *CrystEngComm* **2014**, *16*, 9299–9307. [CrossRef]
23. Khan, S.Z.; Zia-ur-Rehman; Butler, I.S.; Bélanger-Gariepy, F. New ternary palladium(II) complexes: Synthesis, characterization, in vitro anticancer and antioxidant activities. *Inorg. Chem. Commun.* **2019**, *105*, 140–146. [CrossRef]
24. Poirier, S.; Rahmani, F.; Reber, C. Large d–d luminescence energy variations in square-planar bis(dithiocarbamate) platinum(II) and palladium(II) complexes with near-identical MS_4 motifs: A variable-pressure study. *Dalton Trans.* **2017**, *46*, 5279–5287. [CrossRef] [PubMed]
25. Poirier, S.; Roberts, R.J.; Le, D.; Leznoff, D.B.; Reber, C. Interpreting effects of structure variations induced by temperature and pressure on luminescence spectra of platinum(II) bis(dithiocarbamate) compounds. *Inorg. Chem.* **2015**, *54*, 3728–3735. [CrossRef]
26. Imran, M.; Zia-ur-Rehman; Kondratyuk, T.; Bélanger-Gariepy, F. New ternary platinum(II) dithiocarbamates: Synthesis, characterization, anticancer, DNA binding and DNA denaturing studies. *Inorg. Chem. Commun.* **2019**, *103*, 12–20. [CrossRef]
27. Gupta, A.N.; Singh, V.; Kumar, V.; Rajput, A.; Singh, L.; Drew, M.G.B.; Singh, N. Syntheses, crystal structures and conducting properties of new homoleptic copper(II) dithiocarbamate complexes. *Inorg. Chim. Acta* **2013**, *408*, 145–151. [CrossRef]
28. Lanfredi, A.M.M.; Ugozzoli, F.; Camus, A. X-ray crystal structure of the copper(II)bis(2,2′-dipyridyl)dithiocarbamate, produced by an unusual reaction of CS_2 with Cu−N bonds. *J. Chem. Crystallogr.* **1996**, *26*, 141–145. [CrossRef]
29. Rajput, G.; Singh, V.; Singh, S.K.; Prasad, L.B.; Drew, M.G.B.; Singh, N. Cooperative metal–ligand-induced properties of heteroleptic copper(I) xanthate/dithiocarbamate PPh_3 complexes. *Eur. J. Inorg. Chem.* **2012**, 3885–3891. [CrossRef]
30. Gupta, A.N.; Singh, V.; Kumar, V.; Prasad, L.B.; Drew, M.G.B.; Singh, N. Syntheses, crystal structures and optical properties of heteroleptic copper(I) dithio/PPh_3 complexes. *Polyhedron* **2014**, *79*, 324–329. [CrossRef]

31. Singh, A.K.; Yadav, C.L.; Mishra, K.B.; Singh, S.K.; Gupta, A.N.; Tiwari, V.K.; Drew, M.G.B.; Singh, N. Highly efficient and recyclable pre-catalysts based on mono- and dinuclear heteroleptic Cu(I) dithio-PPh_3 complexes to produce variety of glycoconjugate triazoles. *Mol. Catal.* **2019**, *470*, 152–163. [CrossRef]
32. Kumar, V.; Singh, V.; Gupta, A.N.; Manar, K.K.; Prasad, L.B.; Drew, M.G.B.; Singh, N. Influence of ligand environment on the structure and properties of silver(I) dithiocarbamate cluster-based coordination polymers and dimers. *New J. Chem.* **2014**, *38*, 4478–4485. [CrossRef]
33. Roberts, R.J.; Bélanger-Desmarais, N.; Reber, C.; Leznoff, D.B. The luminescence properties of linear vs. kinked aurophilic 1-D chains of bis(dithiocarbamato)gold(I) dimers. *Chem. Commun.* **2014**, *50*, 3148–3150. [CrossRef] [PubMed]
34. Han, S.; Jung, O.-S.; Lee, Y.-A. Adduct effects on structure and luminescence in a series of new dithiocarbamatogold(I) complexes. *Transit. Met. Chem.* **2011**, *36*, 691–697. [CrossRef]
35. Singh, V.; Kumar, V.; Gupta, A.N.; Drew, M.G.B.; Singh, N. Effect of pyridyl substituents leading to the formation of green luminescent mercury(II) coordination polymers, zinc(II) dimers and a monomer. *New J. Chem.* **2014**, *38*, 3737–3748. [CrossRef]
36. Kumar, V.; Manar, K.K.; Gupta, A.N.; Singh, V.; Drew, M.G.B.; Singh, N. Impact of ferrocenyl and pyridyl groups attached to dithiocarbamate moieties on crystal structures and luminescent characteristics of group 12 metal complexes. *J. Organomet. Chem.* **2016**, *820*, 62–69. [CrossRef]
37. Poplaukhin, P.; Arman, H.D.; Tiekink, E.R.T. A one-dimensional coordination polymer, catena-poly[[[[N-ethyl-N-(pyridin-4-ylmethyl)dithiocarbamato-κ^2S,S′]zinc(II)]-μ_2-N-ethyl-N-(pyridin-4-ylmethyl)dithiocarbamato-κ^3S,S′:N] 4-methylpyridine hemisolvate]. *Acta Crystallogr. Sect. E Cryst. Commun.* **2017**, *72*, 1162–1166. [CrossRef] [PubMed]
38. Manar, K.K.; Neetu; Anamika; Srivastava, P.; Drew, M.G.B.; Singh, N. A new series of heteroleptic Cd(II) diimine-ferrocenyl dithiocarbamate complexes which successfully co-sensitizes TiO_2 photoanode with Ru N719 dye in DSSC. *Chem. Sel.* **2017**, *2*, 8301–8311. [CrossRef]
39. Singh, V.; Kumar, V.; Gupta, A.N.; Drew, M.G.B.; Singh, N. Influence of ligand environments on the structures and luminescence properties of homoleptic cadmium(II) pyridyl functionalized dithiocarbamates. *CrystEngComm* **2014**, *16*, 6765–6774. [CrossRef]
40. Arman, H.D.; Poplaukhin, P.; Tiekink, E.R.T. A two-dimensional coordination polymer: Poly[[bis[μ_2-N-ethyl-N-(pyridin-4-ylmethyl)dithiocarbamato-κ^3N:S,S′]cadmium(II)] 3-methylpyridine monosolvate]. *Acta Crystallogr. Sect. E Cryst. Commun.* **2017**, *73*, 488–492. [CrossRef]
41. Singh, V.; Kumar, A.; Prasad, R.; Rajput, G.; Drew, M.G.B.; Singh, N. The interplay of secondary Hg$\cdots$S, Hg$\cdots$N and Hg$\cdots\pi$ bonding interactions in supramolecular structures of phenylmercury(II) dithiocarbamates. *CrystEngComm* **2011**, *13*, 6817–6826. [CrossRef]
42. Rajput, G.; Yadav, M.K.; Thakur, T.S.; Drew, M.G.B.; Singh, N. Versatile coordination environment and interplay of metal assisted secondary interactions in the organization of supramolecular motifs in new Hg(II)/PhHg(II) dithiolates. *Polyhedron* **2014**, *69*, 225–233. [CrossRef]
43. Yadav, M.K.; Rajput, G.; Gupta, A.N.; Kumar, V.; Drew, M.G.B.; Singh, N. Exploring the coordinative behaviour and molecular architecture of new PhHg(II)/Hg(II) dithiocarbamate complexes. *Inorg. Chim. Acta* **2014**, *241*, 210–217. [CrossRef]
44. Singh, V.; Chauhan, R.; Kumar, A.; Bahadur, L.; Singh, N. Efficient phenylmercury(II) methylferrocenyldithiocarbamate functionalized dye-sensitized solar cells. *Dalton Trans.* **2010**, *39*, 9779–9788. [CrossRef] [PubMed]
45. Manar, K.K.; Rajput, G.; Yadav, M.K.; Yadav, C.L.; Kumari, M.; Drew, M.G.B.; Singh, N. Potential impact of substituents on the crystal structures and properties of Tl(I) ferrocenyl/picolyl-functionalized dithiocarbamates; Tl$\cdots$H-C anagostic interactions. *Chem. Sel.* **2016**, *1*, 5733–5742. [CrossRef]
46. Kumar, V.; Singh, V.; Gupta, A.N.; Drew, M.G.B.; Singh, N. Intermolecular Tl$\cdots$H–C anagostic interactions in luminescent pyridyl functionalized thallium(I) dithiocarbamates. *Daltons Trans.* **2015**, *44*, 1716–1723. [CrossRef] [PubMed]
47. Gupta, A.N.; Kumar, V.; Singh, V.; Rajput, A.; Prasad, L.B.; Drew, M.G.B.; Singh, N. Influence of functionalities on the structure and luminescent properties of organotin(IV) dithiocarbamate complexes. *J. Organomet. Chem.* **2015**, *787*, 65–72. [CrossRef]
48. Barba, V.; Arenaza, B.; Guerrero, J.; Reyes, R. Synthesis and structural characterization of diorganotin dithiocarbamates from 4-(ethylaminomethyl)pyridine. *Heteroat. Chem.* **2012**, *23*, 422–428. [CrossRef]
49. Yu, Y.; Yang, H.; Wei, Z.-W.; Tang, L.-F. Synthesis, structure, and fungicidal activity of organotin dithiocarbamates derived from pyridinamines and aryl diamines. *Heteroat. Chem.* **2014**, *25*, 274–281. [CrossRef]
50. Guo, Y.-C.; Ma, Q.-G.; Chen, S.-Y.; Feng, Y.-Q.; Sun, R.-Z. Syntheses, crystal structures and anticancer activities of dithiocarbamate bismuth(III) complexes. *Chin. J. Struct. Chem.* **2015**, *34*, 1028–1034. [CrossRef]
51. Anamika; Singh, R.; Manar, K.K.; Yadav, C.L.; Kumar, A.; Singh, R.K.; Drew, M.G.B.; Singh, N. Impact of substituents on the crystal structures and anti-leishmanial activity of new homoleptic Bi(III) dithiocarbamates. *New J. Chem.* **2019**, *43*, 16921–16931. [CrossRef]
52. Tiekink, E.R.T. Perplexing coordination behaviour of potentially bridging bipyridyl-type ligands in the coordination chemistry of zinc and cadmium 1,1-dithiolate compounds. *Crystals* **2018**, *8*, 18. [CrossRef]
53. Poirier, S.; Lynn, H.; Reber, C.; Tailleur, E.; Marchivie, M.; Guionneau, P.; Probert, M.R. Variation of M$\cdots$H-C interactions in square-planar complexes of nickel(II), palladium(II), and platinum(II) probed by luminescence spectroscopy and X-ray diffraction at variable pressure. *Inorg. Chem.* **2018**, *57*, 7713–7723. [CrossRef]

54. Tiekink, E.R.T. The remarkable propensity for the formation of C–H$\cdots\pi$(chelate ring) interactions in the crystals of the first-row transition metal dithiocarbamates and the supramolecular architectures they sustain. *CrystEngComm* **2020**, *22*, 7308–7333. [CrossRef]
55. Spek, A.L. checkCIF validation ALERTS: What they mean and how to respond. *Acta Crystallogr. Sect. E Cryst. Commun.* **2020**, *76*, 1–11. [CrossRef]
56. Jamaludin, N.S.; Halim, S.N.A.; Khoo, C.-H.; Chen, B.-J.; See, T.-H.; Sim, J.-H.; Cheah, Y.-K.; Seng, H.-L.; Tiekink, E.R.T. Bis(phosphane)copper(I) and silver(I) dithiocarbamates: Crystallography and anti-microbial assay. *Z. Kristallogr.* **2016**, *231*, 341–349. [CrossRef]
57. Tan, Y.J.; Tan, Y.S.; Yeo, C.I.; Chew, J.; Tiekink, E.R.T. In Vitro anti-bacterial and time kill evaluation of binuclear tricyclohexylphosphanesilver(I) dithiocarbamates, $\{Cy_3PAg(S_2CNRR')\}_2$. *J. Inorg. Biochem.* **2019**, *192*, 107–118. [CrossRef] [PubMed]
58. Tiekink, E.R.T.; Kang, J.-G. Luminescence properties of phosphinegold(I) halides and thiolates. *Coord. Chem. Rev.* **2009**, *253*, 1627–1648. [CrossRef]
59. Shattock, R.T.; Arora, K.K.; Vishweshwar, P.; Zaworotko, M.J. Hierarchy of supramolecular synthons: Persistent carboxylic acid···pyridine hydrogen bonds in cocrystals that also contain a hydroxyl moiety. *Cryst. Growth Des.* **2008**, *8*, 4533–4545. [CrossRef]
60. Tiekink, E.R.T. Supramolecular assembly of molecular gold(I) compounds: An evaluation of the competition and complementarity between aurophilic (Au$\cdots$Au) and conventional hydrogen bonding interactions. *Coord. Chem. Rev.* **2014**, *275*, 130–153. [CrossRef]
61. Tiekink, E.R.T. Exploring the topological landscape exhibited by binary zinc-triad 1,1-dithiolates. *Crystals* **2018**, *8*, 292. [CrossRef]
62. Tiekink, E.R.T. Tin dithiocarbamates: Applications and structures. *Appl. Organomet. Chem.* **2008**, *22*, 533–550. [CrossRef]
63. Haezam, F.N.; Awang, N.; Kamaludin, N.F.; Jotani, M.M.; Tiekink, E.R.T. (*N*,*N*-Diallyldithiocarbamato-κ^2S,S')triphenyltin(IV) and bis(*N*,*N*-diallyldithiocarbamato-κ^2S,S')diphenyltin(IV): Crystal structure, Hirshfeld surface analysis and computational study. *Acta Crystallogr. Sect. E Crystallogr. Commun.* **2020**, *76*, 167–176. [CrossRef]
64. Li, H.; Lai, C.S.; Wu, J.; Ho, P.C.; de Vos, D.; Tiekink, E.R.T. Cytotoxicity, qualitative structure-activity relationship (QSAR), and anti-tumor activity of bismuth dithiocarbamate complexes. *J. Inorg. Biochem.* **2007**, *101*, 809–816. [CrossRef]
65. Lai, C.S.; Tiekink, E.R.T. Prevalence of intermolecular Bi ... S interactions in bismuth dithiocarbamate compounds: $Bi(S_2CNR_2)_3$. *Z. Kristallogr.* **2007**, *222*, 532–538. [CrossRef]
66. Alcock, N.W. Secondary bonding to nonmetallic elements. *Adv. Inorg. Chem. Radiochem.* **1972**, *15*, 1–58. [CrossRef]
67. Liu, Y.; Tiekink, E.R.T. Supramolecular associations in binary antimony(III) dithiocarbamates: Influence of ligand steric bulk, influence on coordination geometry, and competition with hydrogen bonding. *CrystEngComm* **2005**, *7*, 20–27. [CrossRef]
68. Tiekink, E.R.T. Aggregation patterns in the crystal structures of organometallic Group XV 1,1-dithiolates: The influence of the Lewis acidity of the central atom, metal- and ligand-bound steric bulk, and coordination potential of the 1,1-dithiolate ligands upon supramolecular architecture. *CrystEngComm* **2006**, *8*, 104–118. [CrossRef]
69. Tiekink, E.R.T.; Zukerman-Schpector, J. Stereochemical activity of lone pairs of electrons and supramolecular aggregation patterns based on secondary interactions involving tellurium in its 1,1-dithiolate structures. *Coord. Chem. Rev.* **2010**, *254*, 46–76. [CrossRef]